
CHALMERS
UNIVERSITY OF TECHNOLOGY

# Antenna Combiner for Periodic Broadcast V2V Communication Under Relaxed Worst-Case Propagation



Citation for the original published paper (version of record):
Bencheikh Lehocine, C., Ström, E., Brännström, F. (2023). Antenna Combiner for Periodic Broadcast V2V Communication Under Relaxed Worst-Case Propagation. IEEE Transactions on Intelligent Transportation Systems, 24(9): 9817-9834. http://dx.doi.org/10.1109/TITS.2023.3271589

# Antenna Combiner for Periodic Broadcast V2V Communication Under Relaxed Worst-Case Propagation

Chouaib Bencheikh Lehocine, Erik G. Ström, *Fellow, IEEE,* and Fredrik Brännström

***Abstract*—The performance of a previously developed analog combining network (ACN) of phase shifters for periodic broadcast vehicle-to-vehicle (V2V) communication is investigated. The original ACN was designed to maximize the sum of signal-to-noise ratios (SNRs) for $K$ consecutive cooperative awareness messages (CAMs). The design was based on the assumption of a dominant propagation path with an angle of arrival (AOA) that is constant for $K$ messages. In this work, we relax this assumption by allowing the AOA and path-loss (PL) of the dominant path to be time-variant. Assuming a highway scenario with a line of sight (LOS) propagation between vehicles, we use affine approximations to model the time variation of different path quantities, including the PL, the relative distance-dependent phase shift between antennas, and the AOA-dependent far-field function of the antennas. By leveraging these approximations, we analytically derive the ACN sum-SNR as each one of these quantities varies over $K$ CAMs. Moreover, we suggest a design rule for a phase slope that is robust against time variation of the dominant path and optimal under time-invariant conditions. Finally, we validate this design rule using numerical computations and an example of vehicular communication antenna elements.**

## I. Introduction

COOPERATIVE intelligent transportation systems (C-ITS) rely on the exchange of cooperative awareness messages (CAMs) to increase traffic safety and traffic efficiency on roads. CAMs are all-to-all broadcast, periodic packets carrying status information about the dynamics of the disseminating vehicles. Due to the broadcast nature of these messages, vehicles need to have an antenna system with good gain in all directions. This is challenged by the fact that antenna patterns are distorted by factors such as the shape of vehicles, mounting positions, and housing of antennas. These factors cause antennas to have low gains or even blind spots in certain directions [1]–[3]. To alleviate this issue, multiple antennas with contrasting patterns can be processed to enable omnidirectional coverage [1], [3]. The use of multiple antennas in the context of vehicular communication has been investigated in several works in the literature. In particular, the classical digital combining schemes, selection combining (SC) and maximal ratio combining (MRC), have been used in [4] to combine antennas mounted on different positions on a vehicle. The schemes were shown to improve the coverage and diversity gain of the antenna system compared to using a single antenna. Similarly, field tests in [5] have shown that MRC and an ideal beam selection receive beamforming yield improved received signal strength compared to a single antenna system.

Besides the aforementioned digital techniques, low-cost analog multiple antenna systems have also been considered for vehicle-to-vehicle (V2V) communication in works, such as [6] and [7]. In [6], a reconfigurable electronically switched parasitic array radiator (ESPAR) antenna system has been proposed. This system can be configured to have an omnidirectional, backward, or forward-directional pattern using a single radio frequency (RF) chain and a control signal. The analog ESPAR system combined with digital MRC was shown in [6] to yield an improved signal-to-noise ratio (SNR) with respect to using MRC alone. In [7], on the other hand, an analog combining network (ACN) of phase shifters has been proposed to mitigate the vehicle-body distortions and enable omnidirectional coverage at the receive side. ACN is a low-cost, low-complexity solution that does not rely on channel state information (CSI) or any control signal from the receiver. In [8], the fully analog ACN combining was enhanced using an MRC-based digital stage to form a hybrid combiner. Then, two transmit-side schemes that are compatible with ACN have been proposed in [9]. The two schemes are an analog beamforming network (ABN) of phase shifters and an antenna switching network (ASN), which periodically alternates between the transmit antennas. Just as for ACN, ABN and ASN do not require CSI and are fully analog. Hence, they have lower complexity than digital schemes, such as cyclic delay diversity (CDD) [10] and Alamouti [11].

To assess the performance of the multiple antenna schemes in [7]–[9], burst error probability (BrEP) was used. BrEP reflects the reliability at the level of C-ITS applications, where an outage occurs if the information about a certain vehicle at a receiving end becomes outdated after the loss of $K$ consecutive CAMs. Using certain assumptions, minimizing BrEP is found in [7]–[9] to be equivalent to maximizing the sum-SNR of $K$ consecutive packets. While ASN does not have any tunable design parameters, to ensure robust V2V communication, phase slopes for ACN and ABN were derived assuming a worst-case propagation environment. This corresponds to a single dominant path with an angle of arrival (AOA) and an angle of departure (AOD) that are assumed to be negligibly varying over $K$ consecutive packets. Additionally, the distance-dependent relative phase shifts between antennas

This research has been carried out in the antenna systems center *ChaseOn* in a project financed by the Swedish Governmental Agency of Innovation Systems (Vinnova), Chalmers, Bluetest, Ericsson, Keysight, RISE, Smarteq, and Volvo Cars.

The authors are with the Communication Systems Group, Department of Electrical Engineering, Chalmers University of Technology, 412 96 Gothenburg, Sweden (e-mail: chouaib@chalmers.se; erik.strom@chalmers.se; fredrik.brannstrom@chalmers.se)

and the path-loss (PL) were also assumed to be negligibly varying over the same duration. A set of optimal phase slopes that maximize the sum-SNR of $K$ consecutive CAMs when the dominant path direction coincides with the worst-case AOA and AOD of the antenna systems were derived in [7], [9].

The negligibly varying single dominant path assumption holds under certain positions and speeds of the transmitter (Tx) and the receiver (Rx), as well as potential reflecting objects. Therefore, we aim to investigate the performance of the optimal phase slopes when the geometries between the Tx and the Rx and their mobility result in a time-varying single dominant path instead of a constant one. Our objective is to assess the sum-SNR of the designed multiple antenna systems when the AOA, AOD, relative phase shifts between the antennas, and PL are time-varying over $K$ packets. This allows us to understand the performance of the derived phase slopes when the worst-case propagation assumption does not fully hold. Furthermore, it guides us to derive design rules to pick phase slopes that are performing well under dynamic scenarios.

The optimal phase slopes under worst-case propagation assumption [7], [9] are available for a generic $L_{\mathrm{s}} \times L_{\mathrm{r}}$ where an ABN or an ASN is used at the Tx with $L_{\mathrm{s}}$ transmit antennas, and an ACN is used at the Rx with $L_{\mathrm{r}}$ receive antennas. However, for such a system, it is difficult to model, analytically study, and understand the effects of time variation of the AOA, AOD, relative phase shift between antennas, and PL. Therefore, we study the effects of these quantities for a $1 \times 2$ ACN system, which is equivalent to studying a $2 \times 1$ ABN system. Since an ASN does not rely on phase shifters, it is not affected by the time variation of the dominant path when used in combination with a single receive antenna. Therefore, we do not include ASN in the analysis below.

To study the $1 \times 2$ ACN, we first use affine functions to approximate the time variation of the dominant path quantities at medium and large distances between the Tx and the Rx. We base this approximation on a reference highway scenario with a line of sight (LOS) propagation, taking into account antenna separation, speeds, as well as distances. Note that a dominant path is not necessarily a LOS, it can be a reflected path too. However, for simplicity, we assume a LOS propagation. Second, we derive an analytical expression for the loss in sum-SNR incurred on the ACN system when the dominant path quantities are time-varying. Third, we derive a design rule to choose a robust phase slope that sustains good performance when the AOA, phase shifts, and PL vary over $K$ CAMs. Finally, using numerical computation, we visualize the performance of the ACN and validate the design rule.

A summary of the contributions of this paper follows.

- Based on a reference highway scenario, where distance, speed, and antenna separation are taken into account, we model the time variation of phase shifts between antennas, PL, and AOA-dependent antenna responses using affine functions.
- We analytically derive the loss function in ACN sum-SNR when the three quantities vary separately.
- We establish a design rule to choose a robust phase slope against the effects of the time variation of the single dominant component quantities.
- Using numerical computation, we validate the design rule and illustrate the performance of ACN under time-varying AOA, phase shifts, and PL.

The investigation of the $1 \times 2$ ACN system is crucial for understanding the effect of time variations. It can be applied to an $L_{\mathrm{s}} \times 2$ system where an ASN is used at the Tx and ACN at the Rx. By viewing this system as $L_{\mathrm{s}}$ parallel $1 \times 2$ subsystems, we can use the $1 \times 2$ ACN analysis (with slight modifications) to gain insights about robust phase slopes for this setup. Moreover, the study performed in this work serves as a guideline for investigating the performance of general $L_{\mathrm{s}} \times L_{\mathrm{r}}$ systems. For these systems, the loss functions in sum-SNR, which seem analytically intractable, can be numerically evaluated and a design rule for robust phase slopes can be devised.

The rest of the paper is organized as follows. In Section II, we give a brief overview of the ACN and ABN, present the system model, and review the main analytical results in [7], [9] needed for the analysis in this paper. In Section III, we present the reference highway scenario along with the different parameters used when modeling the time-varying dominant path. The analysis is then conducted in three successive sections. We investigate the time variation effects of the phase shift between antennas, PL, and AOA on the ACN/ABN[1] in Section IV, Section V, and Section VI, respectively. Numerical results are subsequently presented in Section VII. Finally, we conclude the paper in Section VIII.

## II. Preliminaries

In this section, we briefly reintroduce the ACN and ABN and restate the worst-case propagation assumptions used to design them alongside the obtained optimal phase slopes in [7], [9].

### A. Multiple Antenna Scheme

Consider the multiple antenna scheme shown in Fig. 1 with analog time-varying phase shifters that are modeled following

$$\mathrm{e}^{\jmath(\alpha_l t+\beta_l)}, \quad 0 \leq l \leq L-1, \tag{1}$$

where $\alpha_l \in \mathbb{R}$, and $\beta_l \in [0, 2\pi)$ denote the phase slope and the initial unknown phase offset, respectively, and $L$ is the number of antennas. The scheme is referred to as ACN when used at the Rx and ABN when used at the Tx. A multiplier of $1/\sqrt{L}$ is introduced in (1) to ensure equal transmitted power with respect to a single transmit antenna case when the scheme is used at the transmitter.

### B. Data Traffic Model and Performance Metric

Consider a periodic traffic of CAMs broadcasted by vehicular users (VUs) every $T$ s, where $0.1 \leq T \leq 1$ s [12].

[1] ACN/ABN is used throughout the paper to denote the interchangeability and equivalence between studying ACN at the Rx and ABN at the Tx, when used in combination with a single antenna at the other side.

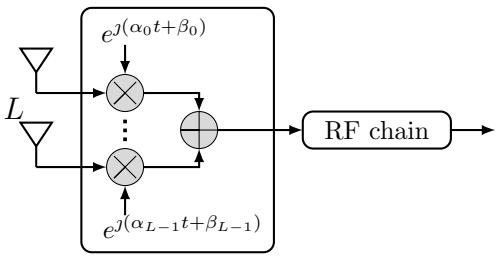


Fig. 1. ACN with $L$ receive antennas.

CAMs carry status information like position, speed, heading, etc. Their repetition interval, $T$, depends on how fast the dynamics of a vehicle are changing, the channel load, and the requirements of C-ITS applications [12]. CAMs are short packets with sizes ranging from 100 to 500 bytes [13]. Assuming IEEE802.11p as an access technology and 6 Mbit/s data rate, their duration satisfies $T_{\mathrm{m}} < 0.7$ ms. (For LTE-V2X technology, the CAM duration corresponds to a subframe duration $T_{\mathrm{m}} = 1$ ms [14].) Observe that the CAM duration is much smaller than the repetition interval $T$, $T_{\mathrm{m}} \ll T$, and this will be used to assert certain assumptions in the sections to come.

Consider that age-of-information (AoI) [15] is used to assess the reliability of a C-ITS application that relies on the information carried by CAMs. At a receiving VU, if the available information about a certain neighboring vehicle has not been updated within a maximum tolerable AoI, $A_{\max}$, then the C-ITS application running at the receiving VU experiences an outage. If latency between the transmission and reception of packets is neglected, an outage occurs if a burst of $K$ consecutive CAMs is lost, implying that $A_{\max} = KT$. The loss of $K$ consecutive packets was defined as the BrEP in [7], and used in [7], [9] as a design metric for ACN and ABN. In particular, the multiple antenna schemes were designed to minimize the BrEP. Under the assumption[2] that packet error probability follows an exponential function of SNR and that packet errors are statistically independent, minimizing the BrEP is found to be equivalent to maximizing the sum of SNR of the $K$ consecutive packets [7, Section III], [8, Section III.B]. Therefore, the sum-SNR is the metric used in assessing the ACN/ABN performance in this paper.

### C. Channel Model and Worst-Case Propagation Scenario

To ensure robust communication, ACN and ABN were designed assuming an environment with scarce multipath propagation. This environment is characterized by a dominant path and a few diffuse components with a small angular spread. A scenario that is typical on highways and roads that are not surrounded by buildings [16]. Such a scenario poses challenges for antenna systems, particularly when the AOD and AOA of the dominant path coincide with directions where the antenna systems have low gain. In these cases, packets can be lost. Additionally, in the cases when the AOD and the AOA are approximately non-varying over $K$ consecutive packets, there is a risk of an outage, i.e., the loss of $K$ consecutive packets. Following this, the baseband channel between the Tx and the Rx was modeled in [7], [9] based on a single dominant physical path. Assuming a $1 \times L$ ACN system (this is equivalent to an $L \times 1$ ABN), the channel gain is given by [17, Ch. 6]

$$h_l(t) = a(t) g_l(\phi) \mathrm{e}^{-\jmath \Omega_l(t)}, \quad l = 0, \ldots, L-1, \tag{2}$$

where $a(t)$ is the (complex) path amplitude, $\phi$ is the AOA, $g_l$ is the far-field function of the receive antenna $l$ in the azimuth plane, and $\Omega_l$ is the relative phase shift at antenna $l$ with respect to the reference antenna with index $l = 0$. It is given by

$$\Omega_l(t) = 2\pi/\lambda (d_l(t) - d_0(t)), \tag{3}$$

where $d_l(t)$ is the propagation distance between the receive antenna with index $l$ and the transmit antenna, and $\lambda$ is the carrier wavelength. Note that $\Omega_0(t) = 0$. The far-field function of the transmit antenna, which can be accounted for by $a(t)$, is assumed for simplicity to be isotropic throughout the paper, and thus $a(t)$ models solely the amplitude of the dominant path.

Since a dominant path with a negligibly varying $\phi$ results in a higher risk of an outage, it is assumed in [7], [9] that the speed and position of the Tx and the Rx, along with potential interacting objects, are such that $\phi$ is approximately constant over the duration of $KT$ s. Consequently, $\Omega_l$ and PL are also assumed to be approximately constant over $KT$ s. These are referred to as the worst-case propagation assumptions, and they were used when designing ACN/ABN.

### D. Sum-SNR Under Worst-Case Propagation

Given the transmission of a CAM, using (1) and (2), the received signal by a VU after ACN combining (as shown in Fig. 1) is expressed as

$$r(t) = a(t)x(t) \sum_{l=0}^{L-1} g_l(\phi) \mathrm{e}^{-\jmath(\Omega_l - \alpha_l t - \beta_l)} + \sum_{l=0}^{L-1} n_l(t), \tag{4}$$

where $x(t) = \tilde{x}(t - \tau(t))$, $\tilde{x}(t)$ is the transmitted baseband signal, $\tau(t) = 2\pi d_0(t)/\lambda$ is the propagation delay, and $n_l(t)$ is an independent zero-mean additive white Gaussian noise over the signal bandwidth with variance $\sigma_{\mathrm{n}}^2$. To express the SNR, we let $P_{\mathrm{r}} = \mathbb{E}\{|a(t)x(t)|^2\}$ denotes the average received power, which is the same for the $K$ packets since the PL is assumed to be constant over $KT$ s. Moreover, we let

$$\psi_l(t) \triangleq \Omega_l(t) - \underline{/g_l(\phi)} - \beta_l, \tag{5}$$

which is non-varying over $KT$ s since $\Omega_l(t)$ is assumed to be non-varying over the same duration. Note that the time variable is dropped for $\psi_l(t)$ and $\Omega_l(t)$, as done, for instance, in (4), whenever $\Omega_l(t)$ is assumed constant. Then, using (4) and (5), we express the SNR of the $k^{\text{th}}$ packet as

$$\gamma_k = \frac{P_{\mathrm{r}}}{L\sigma_{\mathrm{n}}^2} \left| \sum_{l=0}^{L-1} |g_l(\phi)| \mathrm{e}^{-\jmath(\psi_l - \alpha_l kT)} \right|^2, \tag{6}$$

where the phase variation is assumed negligible over a packet duration since $T_{\mathrm{m}} \ll T$, and thus the approximation

[2]Motivation and justification can be found in [9, Section III].

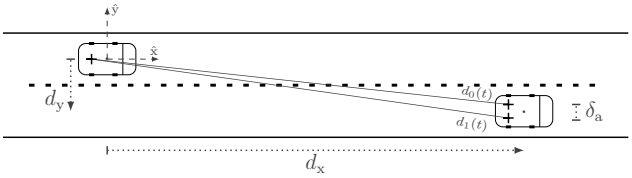


Fig. 2. Two-lane highway scenario with two reference vehicles.

$\mathrm{e}^{-\jmath(\psi_l-\alpha_l t)} \approx \mathrm{e}^{-\jmath(\psi_l-\alpha_l kT)}$ when $kT \le t \le kT+T_\mathrm{m}$, is employed when deriving $\gamma_k$. Then, we can readily express the normalized sum-SNR with respect to $P_\mathrm{r}/\sigma_\mathrm{n}^2$ using the column vectors $\boldsymbol{\alpha} = [\alpha_0, \alpha_1, \ldots, \alpha_{L-1}]^\mathsf{T}$ and $\boldsymbol{\psi} = [\psi_0, \psi_1, \ldots, \psi_{L-1}]^\mathsf{T}$, as

$$\begin{aligned} S(\phi, \boldsymbol{\alpha}, \boldsymbol{\psi}) &= \sigma_\mathrm{n}^2/P_\mathrm{r} \sum_{k=0}^{K-1} \gamma_k \\ &= K \sum_{l=0}^{L-1} \frac{|g_l(\phi)|^2}{L} + J(\phi, \boldsymbol{\alpha}, \boldsymbol{\psi}), \end{aligned} \tag{7}$$

where

$$\begin{aligned} J(\phi, \boldsymbol{\alpha}, \boldsymbol{\psi}) = \frac{2}{L} \sum_{l=0}^{L-2} \sum_{m=l+1}^{L-1} |g_l(\phi)||g_m(\phi)| \\ \times \sum_{k=0}^{K-1} \cos\big(\psi_m - \psi_l - (\alpha_m - \alpha_l)kT\big). \end{aligned} \tag{8}$$

To design ACN/ABN, an optimization problem is defined in [7], [9] to find the phase slopes that maximize the sum-SNR for the worst-case AOA/AOD, and for the worst-case $\boldsymbol{\psi}$ since it depends on the initial unknown and uncontrollable phase offsets $\{\beta_l\}$. The solution to the optimization problem is found in [7], [9] to be the same for any AOA/AOD, and it is given by

$$S^\star(\phi) = \sup_{\boldsymbol{\alpha} \in \mathbb{R}^L} \inf_{\boldsymbol{\psi} \in [0, 2\pi]^L} S(\phi, \boldsymbol{\alpha}, \boldsymbol{\psi}) = K \sum_{l=0}^{L-1} \frac{|g_l(\phi)|^2}{L}. \tag{9}$$

The optimal phase slopes are independent of the far-field functions of antennas and exist when $L \le K$ [7], [9]. They satisfy

$$(\alpha_m - \alpha_l)T/2 \in \mathcal{X}^*, \quad 0 \le l < m \le L-1, \tag{10}$$

where

$$\mathcal{X}^* \triangleq \{q\pi/K : q \in \mathbb{Z}\} \setminus \mathcal{X}, \quad \mathcal{X} \triangleq \{q\pi : q \in \mathbb{Z}\}. \tag{11}$$

The condition in (10) can be satisfied when $L = 2$ using a single phase shifter, where $\alpha_0 = \beta_0 = 0$, and $\alpha_1 T/2 \in \mathcal{X}^*$, $\beta_1 \in [0, 2\pi)$.

## III. Time-Varying Single Dominant Path Propagation

The optimal phase slopes for ACN/ABN were designed under the worst-case assumption of a negligibly varying single dominant path over $KT$ s. In the following, we aim to investigate the effects of time variation of the dominant path on ACN/ABN performance. That is done following an investigation of the impact of variation of $\phi$, $\Omega_l$, and PL separately. Moreover, we aim to define a

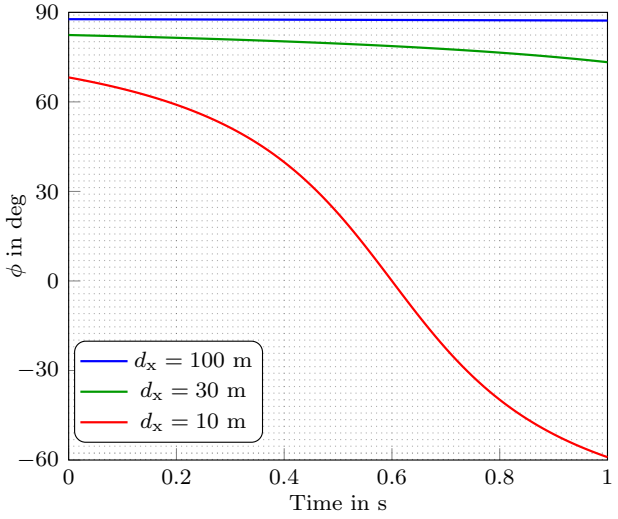


Fig. 3. Time variation of $\phi$ for different initial distances between the Tx and the Rx, $\Delta_\mathrm{v} = -60$ km/h, $d_\mathrm{y} = -4$ m.

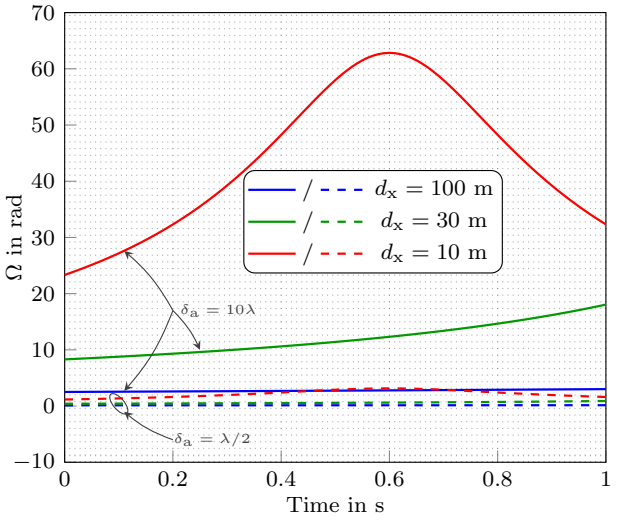


Fig. 4. Time variation of $\Omega_1$ for different initial distances between the Tx and the Rx, $\Delta_\mathrm{v} = -60$ km/h, $d_\mathrm{y} = -4$ m.

design rule to pick a robust phase slope to the variation of these quantities. To be able to perform an analytical investigation of the variation of $\phi$, $\Omega_l$, and PL, we resort to the simple scheme of a $1 \times 2$ system. It allows us to accurately understand the effects of the quantities and to draw design methodology. These can be used as guidelines when investigating the time variation effects of these quantities on $L_\mathrm{s} \times L_\mathrm{r}$, where an ABN is used at the Tx in combination with an ACN at the Rx.

To model the variation of $\phi$, $\Omega_l$, and PL and to evaluate the sum-SNR of the multiple-antenna scheme, we consider two reference VUs on a highway as shown in Fig. 2, one employing two antennas $L = 2$ and it is referred to as the receiving VU, and the other is employing a single antenna, and it is referred to as the transmitting VU. We assume a LOS propagation between the two VUs, which corresponds to the dominant component. If the two VU are moving at the same speed, then the worst-case propagation assumptions in Section II-C (non-variation of the channel) are fully satisfied. In addition, if the two vehicles are

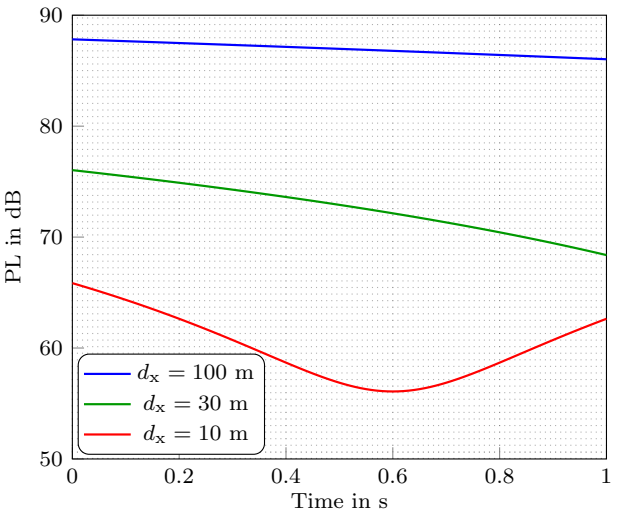


Fig. 5. Time variation of PL following WINNER+B1 path-loss model [18] for different initial distances between the Tx and the Rx, $\Delta_v = -60$ km/h, $d_y = -4$ m.

moving at different speeds but in the same lane, then the AOA and $\Omega_l$ are fixed, while the PL varies. However, if the vehicles are moving at different speeds and located on different lanes, then the geometries between the Tx and the Rx change over time and result in variations of all three quantities of interest. In other words, the accuracy of the aforementioned worst-case scenario assumptions depends on the speed and lane position of vehicles (for this particular scenario). The use of such a scenario allows us to model the variations of the three quantities of interest.

To define certain parameters for the scenario in Fig. 2, we take the initial position of the transmitting VU as the origin $(0, 0)$ of a Cartesian coordinates system. Then, we define the following parameters.

- $d_x$, the initial longitudinal position of the receiving VU with respect to the transmitting VU (measured from the center of vehicles).
- $d_y$, the lateral position of the receiving VU with respect to the transmitting VU.
- $\Delta_v = (v_r - v_t)$, the speed difference between the receiving and the transmitting VUs.
- $\delta_a$, the receive antennas separation.

For simplicity, we assume that the antennas of the Rx are mounted along the lateral axis of the vehicle.

The defined parameters $d_x$, $d_y$, $\Delta_v$, and $\delta_a$ can span a wide range of values. However, we limit the range of these parameters to intervals that are large enough to allow us to observe the different effects resulting from changing geometries between the Tx and the Rx. In particular, we set $d_x \in [-100, 100]$ m since for larger distances than 100 m, $\phi$, $\Omega_l$, and PL are approximately non-varying over $KT$ s. From another aspect, taking into account typical cruising speeds on highways and assuming a maximum regulatory speed of 100 km/h, we can restrict $\Delta_v = (v_t - v_r) \in [-60, 60]$ km/h, which corresponds to absolute speeds in the range $[70, 130]$ km/h. Furthermore, to cover different lane positions, we use $d_y \in [-4, 0, 4]$ corresponding to a lane width of 4 m. Lastly, we consider two cases for $\delta_a$, $\delta_a = \lambda/2 \approx 0.025$ m and $\delta_a = 10\lambda \approx 0.5$ m at carrier frequency $f_c = 5.9$ GHz, corresponding to a small and large antenna separation, respectively.

In Figs. 3–5, we show examples of the time variation of the three quantities for different $d_x$ when $d_y = -4$ m, and $\Delta_v = -60$ km/h, which is the speed within $[-60, 60]$ km/h that results in the maximum change of the quantities. From the figures, we observe that at $d_x = 100$ m, the AOA exhibits negligible change, and so does $\Omega_1$ ($\Omega_0 = 0$) and the PL, implying that the worst-case assumptions in Section II-C hold. At a short distance $d_x = 10$ m, $\phi$ is very rapidly changing. Thus, even if the AOA for a received packet coincides with a low gain of the antenna system, the AOA for the successive packets (e.g., when $T = 0.1$ s) can be coinciding with a high gain of the antenna system, which lowers the risk of consecutive packet losses. More importantly, the PL is very low at such short distances, as seen in Fig. 5, which results in a high SNR and a high probability of decoding packets. Thus, this region is not critical for the communication system.

At the medium distance $d_x = 30$ m, the AOA is slowly changing, with an approximate rate of 9 deg /1 s. In this case, if the AOA for a received packet coincides with a low gain of the antenna system, there is a risk that several successive packets (e.g., when $T = 0.1$ s, $\phi$ changes by 0.9 deg/$T$) experience comparably low gain as well. The PL, which is also slowly changing, is neither too high nor too low in this region. Therefore, there is a risk of losing a burst of consecutive packets due to the alignment of the dominant path with a direction of low gain of the antenna system. From another aspect, the change in $\Omega_1$ is fast (greater than $2\pi$ rad/1 s for $\delta_a = 10\lambda$), which impacts the ACN/ABN system by introducing a time-varying phase offset to the preset phase shifters. Proper antenna processing is of paramount importance in this region of medium to large distances, and it will, therefore, be the focus of the coming analytical investigations.

In the coming three sections, we investigate the effects of time variation of $\phi$, $\Omega_l$, and PL on ACN/ABN performance. When $\phi$ changes, there is a change in the channel phase shift which is captured by $\Omega_l$, and a change in antenna far-field functions $g_l(\phi)$, in both phase and amplitude. When we refer to the time variation effects of $\phi$, we mean the far-field functions variation effects. To simplify the analysis, we study the effects of time variation of each quantity separately. We start with $\Omega_l$, followed by PL, and finally $\phi$. As mentioned earlier, the focus of the analysis is on medium to large distances. This will be backed up by a numerical assessment of the system performance at short distances in the numerical results section.

## IV. Channel Phase ($\Omega$) Variation Effects

In this section, we first model $\Omega_l$ based on the reference scenario shown in Fig. 2 when the distance between the two VUs is medium to large. We then derive the sum-SNR of $1 \times 2$ ACN system under the effects of time variation of $\Omega_l$. Last, we derive a design rule to pick a robust phase slope under these conditions.

### A. Channel Phase Shift ($\Omega$) Model

Given that $L = 2$, and $\Omega_0(t) = 0$, under LOS propagation between the reference VUs shown in Fig. 2, the relative phase shift at receive antenna $l = 1$ with respect to the reference antenna ($l = 0$), $\Omega_1(t) \triangleq \Omega(t)$ is modeled by

$$\begin{aligned}\Omega(t) &= 2\pi/\lambda(d_1(t) - d_0(t)) \\ &= 2\pi/\lambda\Bigg(\sqrt{(d_\mathrm{x} + \Delta_\mathrm{v} t)^2 + (d_\mathrm{y} - \delta_\mathrm{a}/2)^2} - \\ &\qquad \sqrt{(d_\mathrm{x} + \Delta_\mathrm{v} t)^2 + (d_\mathrm{y} + \delta_\mathrm{a}/2)^2}\Bigg). \end{aligned} \tag{12}$$

Observe that as $d_\mathrm{x}$ becomes large $\Delta_\mathrm{v}/d_\mathrm{x} \to 0$, and $\Omega$ becomes approximately constant as seen in Fig. 4. Moreover, the smaller the antenna separation $\delta_\mathrm{a}$, the slower the time variation of $\Omega$. To investigate the effect of this time variation, we resort to the approximation

$$\Omega(t) \approx b_\Omega + a_\Omega\ t, \tag{13}$$

where $a_\Omega$ and $b_\Omega$ can be obtained using first-order Taylor series, or the least squares (LS) method. When first-order Taylor expansion around $t = t_0$ is used, $a_\Omega$ is given by

$$\begin{aligned}a_\Omega = \frac{2\pi}{\lambda}\Delta_\mathrm{v}\Bigg(&\frac{(d_\mathrm{x} + \Delta_\mathrm{v} t_0)}{\sqrt{(d_\mathrm{x} + \Delta_\mathrm{v} t_0)^2 + (d_\mathrm{y} - \delta_\mathrm{a}/2)^2}} \\ &- \frac{(d_\mathrm{x} + \Delta_\mathrm{v} t_0)}{\sqrt{(d_\mathrm{x} + \Delta_\mathrm{v} t_0)^2 + (d_\mathrm{y} + \delta_\mathrm{a}/2)^2}}\Bigg), \end{aligned} \tag{14}$$

and $b_\Omega = \Omega(t_0) - a_\Omega t_0$. Based on Fig. 4, we expect the affine approximation to have good accuracy at medium to large distances with $\Delta_\mathrm{v} \in [-60, 60]$ km/h. At short distances, the approximation is not expected to be very accurate, especially when the antenna separation is large (e.g., $\delta_\mathrm{a} = 10\lambda$), and the speed difference is high.

### B. Sum-SNR

To evaluate the sum-SNR of ACN/ABN taking into account the effects of time variation of $\Omega$ only, we assume the use of isotropic antennas at the Rx, i.e., $g_0(\phi) = g_1(\phi) = 1$, $\forall\phi$. Thus, despite that $\phi$ varies, the gain of the antenna system does not vary. Moreover, we assume that PL is approximately non-varying over $KT$ s. This allows us to disentangle the effects of variation of the channel phase $\Omega$ from the effects of variation of AOA and PL. Now, assume that the ACN is implemented using a single phase shifter, implying that $\alpha_0 = \beta_0 = 0$, and $\alpha_1 \triangleq \alpha \in \mathbb{R}$, $\beta_1 \triangleq \beta \in [0, 2\pi)$. Then, from (5) and (13), we have

$$\begin{aligned}\psi_1(t) - \psi_0(t) &= (\Omega(t) - \underline{\angle g_1(\phi)} - \beta) + \underline{\angle g_0(\phi)} \\ &\approx (b_\Omega + a_\Omega\ t - \underline{\angle g_1(\phi)} - \beta) + \underline{\angle g_0(\phi)} \\ &= y + a_\Omega\ t \end{aligned} \tag{15}$$

where

$$y = b_\Omega - \underline{\angle g_1(\phi)} - \beta + \underline{\angle g_0(\phi)}. \tag{16}$$

Assuming that the time variation due to $a_\Omega$ is negligible over a packet duration $T_\mathrm{m} \ll T$, we approximate for $kT \le t \le kT + T_\mathrm{m}$, $k = 0, 1, \ldots, K-1$,

$$\psi_1(t) - \psi_0(t) \approx \psi_1(kT) - \psi_0(kT). \tag{17}$$

Following this, the sum-SNR (7) can be expressed taking into account (15), the isotropic antenna characteristics, and $L = 2$ as

$$S_\Omega(\phi, \boldsymbol{\alpha}, \boldsymbol{\psi}) = \sigma_\mathrm{n}^2/P_\mathrm{r} \sum_{k=0}^{K-1} \gamma_k = K + J_\Omega(\phi, \boldsymbol{\alpha}, \boldsymbol{\psi}), \tag{18}$$

where $J_\Omega$ is given by (8), and it simplifies to

$$\begin{aligned}J_\Omega(\phi, \boldsymbol{\alpha}, \boldsymbol{\psi}) &= |g_0(\phi)||g_1(\phi)| \\ &\quad \times \sum_{k=0}^{K-1} \cos\left(\psi_1(kT) - \psi_0(kT) - (\alpha_1 - \alpha_0)kT\right) \\ &\approx \sum_{k=0}^{K-1} \cos\left(y + a_\Omega kT - \alpha kT\right) \\ &= \sum_{k=0}^{K-1} \cos\left(y - (\alpha - a_\Omega)kT\right) \\ &= \sum_{k=0}^{K-1} \cos\left(y - 2xk\right) \\ &\triangleq J_\Omega(x, y), \end{aligned} \tag{19}$$

where the approximation follows from (15), and where

$$x \triangleq (\alpha - a_\Omega)T/2. \tag{20}$$

We can write the sum-SNR as

$$S_\Omega(x, y) = K + J_\Omega(x, y). \tag{21}$$

Now, we can evaluate the performance of the system using the worst-case sum-SNR, which is similar to what was used in the optimization problem in (9),

$$\inf_{y \in [0, 2\pi)} S_\Omega(x, y) = K\left(1 + \inf_{y \in [0, 2\pi)} \frac{J_\Omega(x, y)}{K}\right). \tag{22}$$

That is, we account for the worst-case value of $y$ since it depends on the unknown, uncontrollable, initial phase shift $\beta$ of the ACN. When the channel phase variations are negligible, $a_\Omega = 0$, we know from (9) that the optimal worst-case sum-SNR is given by $\inf_y S_\Omega(x, y) = K$, which implies that $\inf_y J_\Omega(x, y) = 0$. Therefore, we define the loss function as

$$L_\Omega(x) \triangleq -\inf_{y \in [0, 2\pi)} \frac{J_\Omega(x, y)}{K}, \tag{23}$$

and we characterize some of its properties in the following lemma.

**Lemma 1.** *Let $L_\Omega(x)$ be as defined in (23), $x \in \mathbb{R}$, and let $\mathcal{X}$ be as defined in (11), then*

*(i) The loss function is given by*

$$L_\Omega(x) = \begin{cases} 1, & x \in \mathcal{X} \\ |f_1(x)|/K, & x \notin \mathcal{X} \end{cases} \tag{24}$$

*where $f_1 : \mathbb{R} \setminus \mathcal{X} \to \mathbb{R}$, is given by*

$$f_1(x) = \frac{\sin(Kx)}{\sin(x)}. \tag{25}$$

*(ii) $L_\Omega$ is periodic with period $\pi$, and symmetric around $\pi/2$.*

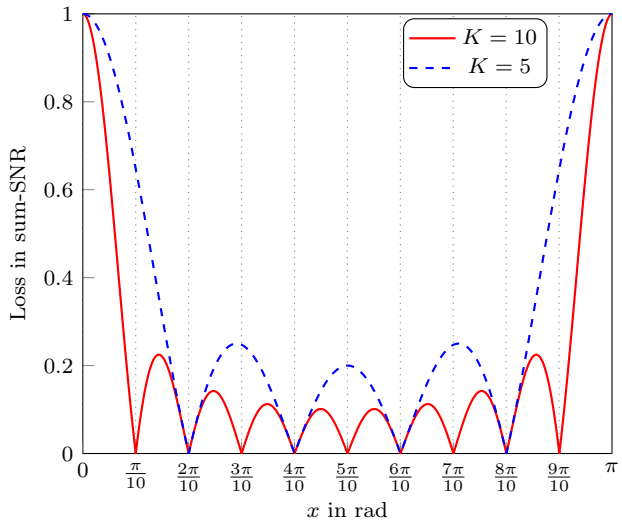


Fig. 6. The sum-SNR loss function $L_\Omega(x)$, $x = (\alpha - a_\Omega)T/2$ when $K = 5, 10$.

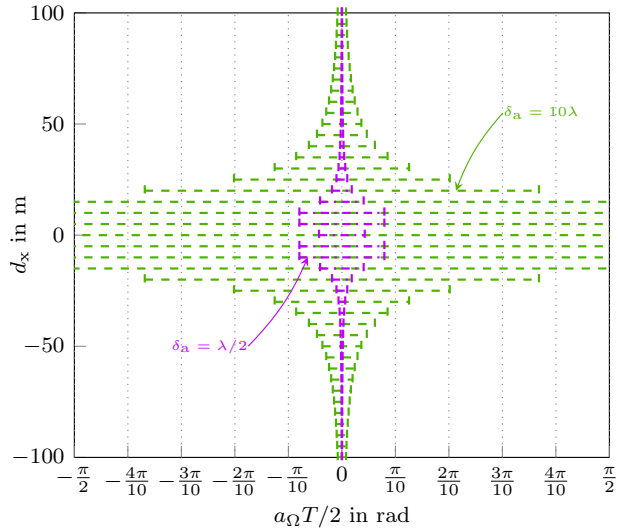


Fig. 7. Range of change in $\Omega$ as a function of $d_x$ when $\Delta_v \in [-60, 60]$ km/h, and $d_y = \pm 4$. First order Taylor expansion (14) is used to compute $a_\Omega$.

*(iii) The loss function is bounded as*

$$0 \leq L_\Omega(x) \leq 1, \quad x \in [0, \pi), \tag{26}$$

*where $L_\Omega(x) = 0$ when $x \in \mathcal{X}^\star$, and $\mathcal{X}^\star$ is defined in (11).*

*Proof.* See the Appendix. □

The loss function for $K = 5$ and $K = 10$ is shown in Fig. 6. Since $L_\Omega(x)$ is periodic with period $\pi$, we define

$$\mathcal{A}^\star \triangleq \left\{ q\frac{2\pi}{KT}; q = 1, 2, \ldots, K-1 \right\}, \tag{27}$$

which has $K - 1$ elements, where each $\alpha \in \mathcal{A}^\star$ satisfies $\alpha T/2 \in \mathcal{X}^\star$. These are all the unique elements in $\mathcal{X}^\star$, since for every $x \in \mathcal{X}^\star$, we can write $x = \alpha T/2 + q\pi$, where $\alpha \in \mathcal{A}^\star$, $q \in \mathbb{Z}$.

Recall that when $a_\Omega = 0$, all $\alpha \in \mathcal{A}^\star$ yield the same optimal sum-SNR, and $L_\Omega(x) = 0$. However, under channel phase variation, $a_\Omega \neq 0$, these phase slopes yield different sum-SNR. To observe that, consider an example where $a_\Omega T/2 \in [-\pi/K, \pi/K]$, and $\alpha T/2 = \pi/K$ ($\alpha \in \mathcal{A}^\star$). It follows that $x = (\alpha - a_\Omega)T/2 \in [0, 2\pi/K]$, and thus, the worst-case loss due to phase deviation $a_\Omega$ corresponds to $L_\Omega(x) = 1$, as can be seen from Fig. 6. On the other hand, when $\alpha T/2 = 2\pi/K$, ($\alpha \in \mathcal{A}^\star$) it follows that $x \in [\pi/K, 3\pi/K]$, and from Fig. 6 we see that the worst-case loss in this case is $L_\Omega(x) \approx 0.25$, and $L_\Omega(x) \approx 0.22$ for $K = 5$, and $K = 10$, respectively. Hence, under channel phase variation, not all phase slopes $\alpha \in \mathcal{A}^\star$ yield the same loss in sum-SNR. Moreover, $\alpha T/2 = 2\pi/K$ is more robust than $\alpha T/2 = \pi/K$ in mitigating phase deviation effects when $a_\Omega T/2 \in [-\pi/K, \pi/K]$. Therefore, in the following, we propose a design rule to choose a robust phase slope in $\mathcal{A}^\star$ under channel phase shift variation.

### C. Phase Slope Design Under Time-Varying $\Omega$ ($a_\Omega \neq 0$)

To derive a design rule to choose a robust phase slope in $\mathcal{A}^\star$ under channel phase variation, we start by characterizing the trends of the loss function, $L_\Omega(x)$. Let $\alpha \in \mathcal{A}^\star$, and assume that $a_\Omega \neq 0$. At the points $x = (\alpha - a_\Omega)T/2 = q\pi$ the loss function is at its maximum value $L_\Omega(x) = 1$. On the other hand, as can be seen in Fig. 6, in the range $[\pi/K, (K-1)\pi/K]$ the loss function exhibits $K - 2$ lobs. These lobes have decreasing maxima in the range $[\pi/K, \pi/2]$. That follows since $\sin(x)$ is increasing over the interval, while $|\sin(Kx)|$ is periodic with $\pi/K$ (which is equal to the lobes width). Due to the symmetry around $\pi/2$, the lobes maxima are increasing as we get far from the symmetry point in the range $[\pi/2, (K-1)\pi/K]$. In addition, the maximum loss within $[\pi/K, (K-1)\pi/K]$ is bounded following

$$L_\Omega(x) \leq \frac{1}{K \sin(\pi/K)}, \quad x \in \left[\frac{\pi}{K}, (K-1)\frac{\pi}{K}\right], \tag{28}$$

since $|\sin(Kx)| \leq 1$ and $\sin(\pi/K) \leq \sin(x)$ where $x \in [\pi/K, (K-1)\pi/K]$. This bound is decreasing with $K$ and it quantifies to $L_\Omega(x) \leq 0.34$ for $K = 5$, and $L_\Omega(x) \leq 0.32$ for $K = 10$. Substituting with the bound in (22) we deduce that the sum-SNR when $x \in [\pi/K, (K-1)\pi/K]$ is at worst $-1.8$ dB, and $-1.7$ dB below the zero-loss sum-SNR ($\inf_y S_\Omega(x, y) = K$) for $K = 5$, and $K = 10$, respectively. Hence, in summary, the loss in sum-SNR is moderate within the interval $[\pi/K, (K-1)\pi/K]$ and it gets lower as we approach the point of symmetry $\pi/2$ of the loss function. On the other hand, the loss in sum-SNR is severe in the intervals centered around the points $(\alpha - a_\Omega)T/2 = q\pi$.

Guided by these trends in the loss function $L_\Omega(x)$, we aim to pick a phase slope in $\mathcal{A}^\star$ that handles a wide range of error due to channel variation, $a_\Omega$, without resulting in the most severe loss in sum-SNR occurring at $x = (\alpha - a_\Omega)T/2 = q\pi$. This is equivalent to picking the phase slope that has the largest phase distance from the points with the most severe loss, $x = q\pi$, and which is, in turn, the phase slope that has the shortest phase distance from the point $x = \pi/2$. We formally define this as

$$\alpha^\star \triangleq \arg\min_{\alpha \in \mathcal{A}^\star} |\alpha T/2 - \pi/2|. \tag{29}$$

Besides having the largest phase distance from the points with the most severe loss, the ACN with $\alpha^\star$ ensures that the effective phase slope $(\alpha^\star - a_\Omega)T/2$ is within the region with moderate loss in sum-SNR, $[\pi/K, (K-1)\pi/K]$ for the widest range of $a_\Omega$ compared to any other phase slope in $\mathcal{A}^\star$. Thus, $\alpha^\star$ is the most robust phase slope in $\mathcal{A}^\star$ when $\Omega$ is time-varying. The solutions to (29) are given by

$$\alpha^\star \in \begin{cases} \left\{ \frac{K}{2}\frac{2\pi}{KT} \right\}, & K \text{ even} \\ \left\{ \frac{K-1}{2}\frac{2\pi}{KT}, \frac{K+1}{2}\frac{2\pi}{KT} \right\}, & K \text{ odd} \end{cases} \tag{30}$$

To get more insight into the design rule (29) we plot in Fig. 7 the range of $a_\Omega$ as a function of $d_\mathrm{x}$ when $\Delta_\mathrm{v} \in [-60, 60]$ km/h. **(i)** We observe that for $\delta_\mathrm{a} = \lambda/2$ the variation of $a_\Omega$ is very limited at medium to large distances. This indicates that the impact of channel phase variation is not severe when the antenna separation is small. **(ii)** For $\delta_\mathrm{a} = 10\lambda$, we see that $a_\Omega$ has much wider range compared to $\delta_\mathrm{a} = \lambda/2$. The interval of $a_\Omega$ increases with the increase of speed difference $|\Delta_\mathrm{v}|$ or the decrease of distance $|d_\mathrm{x}|$. This is an indication that certain choices of $\alpha \in \mathcal{A}^\star$ can have better properties in mitigating the effects of variation of $\Omega$ over a wide range of speeds and distances. This supports the proposed design rule in (29). For example, assuming $K = 10$, then $\alpha^\star T/2 = \pi/2$. Following that, from Fig. 7 we obtain that when $|d_\mathrm{x}| \geq 20$ m, $|a_\Omega|T/2 < \pi/2$ for $\Delta_\mathrm{v} \in [-60, 60]$. Thus, when $|d_\mathrm{x}| \geq 20$, the effective phase slope $(\alpha^\star - a_\Omega)$ satisfies $0 < (\alpha^\star - a_\Omega)T/2 < \pi$, implying that $\alpha^\star$ allows us to avoid severe loss in sum-SNR for any speed when $|d_\mathrm{x}| \geq 20$ m. On the other hand, using $\alpha T/2 = \pi/K$, then $0 < (\alpha - a_\Omega)T/2 < \pi$ is satisfied for any $\Delta_\mathrm{v} \in [-60, 60]$, only when $|d_\mathrm{x}| \geq 35$ m. Hence, for medium distances below 35 m, there exists $\Delta_\mathrm{v} \in [-60, 60]$ for which the ACN system with $\alpha T/2 = \pi/K$ experiences the most severe loss in sum-SNR. Thus, $\alpha^\star$ is a robust choice that allows us to avoid severe loss in sum-SNR over a wide range of distances.

For short distances $|d_\mathrm{x}| \leq 15$ ($\delta_\mathrm{a} = 10\lambda$), we see in Fig. 7 that $a_\Omega T/2$ can take any value in $[-\pi/2, \pi/2]$ (recall that $L_\Omega$ is periodic with $\pi$), which implies that for any $\alpha \in \mathcal{A}^\star$ including $\alpha^\star$, there exists $\Delta_\mathrm{v} \in [-60, 60]$ for which the most severe loss is experienced. In other words, no choice of phase slope is better than others in mitigating the effects of variation of $\Omega$ over the full speed range $\Delta_\mathrm{v} \in [-60, 60]$ at short distances $|d_\mathrm{x}| \leq 15$ ($\delta_\mathrm{a} = 10\lambda$). However, we recall that approximating $\Omega$ as an affine function (13) is not very accurate over the full range of speed difference at low distances. Therefore, a numerical quantification of the system performance at such short distances is shown in the numerical results section.

## V. Path-loss Variation Effects

In this section, we investigate the performance of ACN under time-varying PL following the same steps as in the previous section.

### A. Path-loss Model

The path-loss is typically modeled following a power law [19], and so does its inverse, the path gain, which will be the one explicitly used in the analysis to follow. A generic model of the path gain is given by [19]

$$A(t) = A_0 \times \left(\frac{d_\mathrm{ref}}{d(t)}\right)^{n_\mathrm{e}} 10^{-X_\sigma(d)/10}, \; d \geq d_\mathrm{ref}, \tag{31}$$

where $d(t) = \sqrt{(d_\mathrm{x} + \Delta_\mathrm{v} t)^2 + d_\mathrm{y}^2}$, is the distance between the Tx and the Rx, $n_\mathrm{e}$ is the path loss exponent, $d_\mathrm{ref}$ is a reference distance with path gain $A_0$, and $X_\sigma(d)$ is a zero-mean Gaussian random process with standard deviation $\sigma_\mathrm{SH}$ corresponding to shadowing (large scale fading). Shadowing is a spatially correlated process with autocorrelation $\mathbb{E}\{X_\sigma(d)X_\sigma(d+\Delta d)\}$, that can be modeled using a decaying exponential function with parameter $d_\mathrm{c}$ [20]. The decorrelation distance $d_\mathrm{c}$, represents the distance difference at which the autocorrelation is equal to $\mathrm{e}^{-1}$. In the context of highway scenarios, it is reported to be $23.3 \leq d_\mathrm{c} \leq 32.5$ m in [19], and $d_\mathrm{c} = 25$ m in WINNER+B1 path-loss model [18]. Taking this into account, and for simplicity, we assume that shadowing is a block-type fading over the duration of $KT$s,

$$X_\sigma \triangleq X_\sigma(d|_{t=(K-1)T/2}), \; 0 \leq t \leq KT.$$

Then, assuming that[3] $d(0) > d_\mathrm{ref}$ and $d\big((K-1)T\big) > d_\mathrm{ref}$, we can approximate the average path gain following

$$\overline{A}(t) = \mathbb{E}\{A(t)\} = \mu_X A_0 \left(\frac{d_\mathrm{ref}}{d(t)}\right)^{n_\mathrm{e}} \approx b_\mathrm{PL} + a_\mathrm{PL} t, \tag{32}$$

where $\mu_X = \mathbb{E}\{10^{-X_\sigma/10}\} = \mathrm{e}^{(\ln(10)\sigma_\mathrm{SH})^2/200}$. Assuming that the variation of path gain is negligible over a packet duration $T_\mathrm{m} \ll T$, we reach

$$\overline{A}(t) \approx \overline{A}(kT) = b_\mathrm{PL} + a_\mathrm{PL} kT, \; kT \leq t \leq kT + T_\mathrm{m}.$$

The approximating affine function parameters can be computed using either first-order Taylor expansion or using the LS method. Since $\overline{A}(kT) > 0$, the coefficients need to satisfy the condition $b_\mathrm{PL} + a_\mathrm{PL} kT > 0$, $k = 0, 1, \ldots, K-1$, for the approximation to be valid. When Taylor expansion at $t = t_0$ is applied, the coefficients are given by

$$a_\mathrm{PL} = -\mu_X A_0 d_\mathrm{ref}^{n_\mathrm{e}} \frac{n_\mathrm{e}\Delta_\mathrm{v} \times (d_\mathrm{x} + \Delta_\mathrm{v} t_0)}{d^{n_\mathrm{e}+2}(t_0)}, \tag{33}$$

and $b_\mathrm{PL} = \overline{A}(t_0) - a_\mathrm{PL}\, t_0$.

### B. Sum-SNR

To study the effects of the variation of the average PL on the ACN/ABN system, we assume that the two reference vehicles in Fig. 2 are moving in the same lane, i.e., $d_\mathrm{y} = 0$ m. Hence, the AOA and the channel phase shift do not change with time ($a_\Omega = 0$). Furthermore, we assume that the antennas have isotropic patterns (i.e., even if $\phi$ is time-varying, the antenna responses are fixed).

The received power of the $k^\mathrm{th}$ packet can be expressed as $P_\mathrm{r} = \mathbb{E}\{|a(t)x(t)|^2\} = \overline{A}(kT)P_\mathrm{t}$, where $\overline{A}(kT) =$

[3] When $d < d_\mathrm{ref}$, the model in (31) is invalid. In such a case, the path gain can be assumed to be equal to that at $d_\mathrm{ref}$ as done, for example, in WINNER+B1 model [18, Table A.1.4-1].

$\mathbb{E}\{|a(t)|^2\}$, and $P_{\rm t} = \mathbb{E}\{|x(t)|^2|\}$ is the transmitted power. Then, the SNR of the $k^{\rm th}$ packet (6) is expressed as

$$\gamma_k = \frac{P_{\rm t}}{L\sigma_{\rm n}^2}\overline{A}(kT)\left|\sum_{l=0}^{L-1} \mathrm{e}^{-\jmath(\psi_l - \alpha_l kT)}\right|^2, \tag{34}$$

since $g_l(\phi) = 1$, $l = 0, 1$. Then, normalizing the SNR with respect to $P_{\rm t}/\sigma_{\rm n}^2$ and summing over $k$, we find that

$$\begin{aligned} S_{\rm PL}(x,y) &= \frac{1}{L}\sum_{k=0}^{K-1}\overline{A}(kT)\big(2+2\cos(y-2xk)\big) \\ &\approx \frac{1}{L}\sum_{k=0}^{K-1}(b_{\rm PL}+a_{\rm PL}kT)\big(2+2\cos(y-2xk)\big) \\ &= c_1 K\left(1+\frac{J_{\rm PL}(x,y)}{c_1 K}\right), \end{aligned} \tag{35}$$

where the approximation follows from (32), and where $x$ and $y$ are given by (20) and (16), respectively ($x = \alpha T/2$, since $a_\Omega = 0$), $c_1 = \big(b_{\rm PL} + a_{\rm PL}T(K-1)/2\big)$, and

$$J_{\rm PL}(x,y) = \sum_{k=0}^{K-1}(b_{\rm PL}+a_{\rm PL}kT)\cos\big(y-2xk\big). \tag{36}$$

As done earlier, we define the loss function as

$$L_{\rm PL}(x) \triangleq -\inf_{y\in[0,2\pi)}\frac{J_{\rm PL}(x,y)}{c_1 K}, \tag{37}$$

where the worst-case sum-SNR is given by

$$\inf_{y\in[0,2\pi)} S_{\rm PL}(x,y) = c_1 K(1 - L_{\rm PL}(x)). \tag{38}$$

We then state certain properties of the loss function in the following lemma.

**Lemma 2.** *Let $L_{\rm PL}(x)$ be as defined in (37), $x \in \mathbb{R}$, and $(b_{\rm PL} + a_{\rm PL}kT) > 0$, $k = 0, 1, \ldots, K-1$, then*

*(i) The loss function is given by*

$$L_{\rm PL}(x) = \begin{cases} 1, & x \in \mathcal{X} \\ \sqrt{c_1^2 f_1^2(x) + c_2^2 f_2^2(x)}/(c_1 K), & x \notin \mathcal{X} \end{cases} \tag{39}$$

*where $c_1 = \big(b_{\rm PL} + a_{\rm PL}T(K-1)/2\big)$, $c_2 = a_{\rm PL}T/2$, $\mathcal{X}$ is defined in (11), $f_1$ is defined in (25), and $f_2 : \mathbb{R}\setminus\mathcal{X} \to \mathbb{R}$, is given by*

$$f_2(x) = \frac{K\cos(Kx)}{\sin(x)} - \frac{\sin(Kx)}{\sin(x)}\cot(x). \tag{40}$$

*(ii) The loss function is periodic with period $\pi$ and symmetric around $\pi/2$.*

*(iii) $L_{\rm PL}$ can be bounded as*

$$0 < L_{\rm PL}(x),\ a_{\rm PL} \neq 0, \quad L_{\rm PL}(x) \leq 1. \tag{41}$$

*(iv) If $x \in \mathcal{X}^\star$ then*

$$L_{\rm PL}(x) = \left|\frac{c_2}{c_1\sin(x)}\right|. \tag{42}$$

*(v) The loss function is bounded when $x \notin \mathcal{X}$ as*

$$\frac{|f_1(x)|}{K} \leq L_{\rm PL}(x) \leq \frac{\sqrt{(K-1)^2 f_1^2(x) + f_2^2(x)}}{K(K-1)}. \tag{43}$$

*Proof.* See the Appendix. □

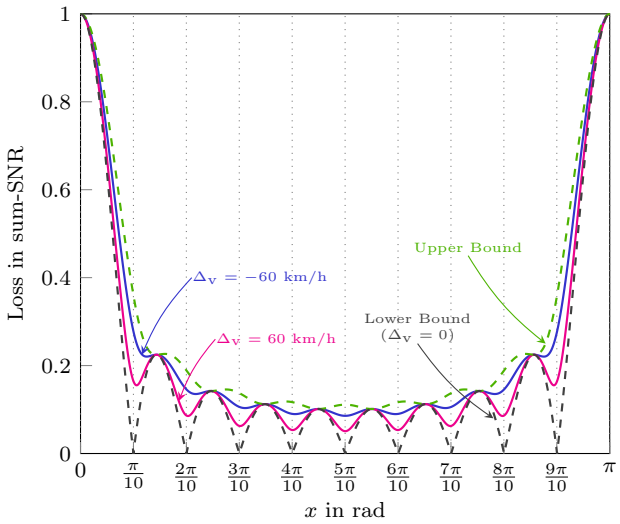


Fig. 8. The sum-SNR loss function under PL variation, $L_{\rm PL}(x)$, for $K = 10$, $d_{\rm x} = 30$ m, $d_{\rm y} = 0$ m, and $\Delta_{\rm v} = \pm 60$ km/h. The upper and lower bounds (43) of the loss function are shown in dashed lines.

### C. Phase Slope Design Under Time-Varying PL ($a_{\rm PL} \neq 0$)

We recall that when the PL is approximated as constant ($a_{\rm PL} = 0$), the phase slopes $x = \alpha T/2 \in \mathcal{X}^\star$ ensure identical optimal performance corresponding to $\inf_y S_{\rm PL}(x,y) = c_1 K$, and $L_{\rm PL}(x) = 0$. Now, when the PL is time-varying, $a_{\rm PL} \neq 0$, we see from Lemma 2 (42) that the loss in sum-SNR $L_{\rm PL}(x) \neq 0$ for $x = \alpha T/2 \in \mathcal{X}^\star$, and it is not identical for all the elements of $\mathcal{X}^\star$. Since $L_{\rm PL}$ is periodic with $\pi$, there exist $K-1$ unique elements in $\mathcal{X}^\star$, which are represented in $\mathcal{A}^\star$ (27). Following that, we can deduce that the phase slope that minimizes the loss in sum-SNR under PL variation among $\mathcal{A}^\star$ is also the solution to (29). That is,

$$\arg\min_{\alpha\in\mathcal{A}^\star} L_{\rm PL}(\alpha T/2) = \arg\min_{\alpha\in\mathcal{A}^\star} |\alpha T/2 - \pi/2|. \tag{44}$$

This follows from (42) since $1/|\sin(\alpha T/2)|$ is minimized by the phase slope satisfying the right-hand side of (44). These results can be observed in Fig. 8 where the loss function, is plotted for $d_{\rm x} = 30$ m and $\Delta_{\rm v} = \pm 60$ km/h. The WINNER+B1 path-loss model [18], [21] is used. Assuming a carrier frequency $f_{\rm c} = 5.9$ GHz, and antenna heights of 1.5 m, the path gain between the Tx and the Rx when $d \leq 177$ m (this distance depends on $f_{\rm c}$ and the antennas heights) can be modeled using (31), with the parameters, $d_{\rm ref} = 3$ m, $A_0 = 10^{5.32}$, $n_{\rm e} = 2.27$, and $\sigma_{\rm SH} = 3$.

From Fig. 8, and using the bounds in (43), we see that the loss in sum-SNR is low for all $\alpha \in \mathcal{A}^\star$ ($x = \alpha T/2 = q\pi/K$). In particular, substituting by the upper bound (43) of the loss function in (38) we can deduce that the phase slopes $\alpha = q2\pi/KT$, where $q = 1, \ldots, K/2$, ($\alpha \in \mathcal{A}^\star$), respectively achieve a sum-SNR that is at worst, $-1.94$, $-0.91$, $-0.64$, $-0.54$, and $-0.51$ dB, lower than the reference zero-loss sum-SNR, $\inf_y S_{\rm PL}(x,y) = c_1 K$. Note that due to the symmetry of the loss function with respect to $\pi/2$, the phase slopes $\alpha = q2\pi/KT$, $q = K/2+1, \ldots, K-1$, achieve identical sum-SNR to their symmetric counterparts.

Thus unlike the effects of variation in $\Omega$, when PL is time-varying over the duration of $KT$ s at medium to large distances, the loss in sum-SNR is much lower than the maximum loss $L_{\mathrm{PL}}(x) = 1$, and thus PL time variation does not cause severe loss in sum-SNR.

As $d_{\mathrm{x}}$ increases, the loss in sum-SNR decreases for all phase slopes $\alpha \in \mathcal{A}^{\star}$. This can be observed from Lemma 2 (42), where the loss is proportional to $c_2/c_1$, which is given by

$$\left|\frac{c_2}{c_1}\right| = \frac{n_{\mathrm{e}}|\Delta_{\mathrm{v}}|}{|d_{\mathrm{x}} + \Delta_{\mathrm{v}} t_0|} T/2, \quad (d_{\mathrm{y}} = 0), \tag{45}$$

assuming the use of (33) with $t_0 = (K-1)T/2$. As $d_{\mathrm{x}}$ becomes large, the loss becomes negligible for all phase slopes $\alpha \in \mathcal{A}^{\star}$.

### D. Combined PL and $\Omega$ Variation

Consider now the scenario where the two reference VUs (in Fig. 2) are on different lanes $d_{\mathrm{y}} \neq 0$. Then, besides PL, $\Omega$ is also time-varying over $KT$ s, and can be approximated using (13), where $a_{\Omega} \neq 0$. Despite that $\phi$ varies too, the isotropic antenna responses are fixed, and do not affect the system. In this scenario, the sum-SNR and the loss function are still modeled by (35) and (37) respectively, where $x = (\alpha - a_{\Omega})T/2$. Therefore, at medium to long distances, variation in PL changes the shape of the loss function, in the sense that, for any $x$, the loss in sum-SNR is greater than the loss under non-varying PL, $L_{\mathrm{PL}}(x) \geq L_{\mathrm{PL}}(x)|_{\Delta_{\mathrm{v}}=0}$, as can be seen in Fig. 8. On the other hand, variation in $\Omega$ deviates the ACN/ABN phase slope $\alpha$ by an offset of $a_{\Omega}$. Using the bounds (43) and from Fig. 8, we see that the loss function under PL variation has similar trends to the loss function under time-varying $\Omega$ (24) (which is the lower bound). That is, the maximum loss occurs at the points $x = (\alpha - a_{\Omega})T/2 = q\pi$, and the loss function has decreasing maxima within $[\pi/K, \pi/2]$, and increasing maxima in $[\pi/2, (K-1)\pi/K]$. Thus, under the variation of both PL and $\Omega$, the design rule (29) still leads to the most robust phase slope in $\mathcal{A}^{\star}$. In other words, choosing a phase slope according to (29) allows us to avoid the most severe loss in sum-SNR over the widest range of $a_{\Omega}$, when both $\Omega$ and PL are time-varying over $KT$ s.

## VI. Effects of AOA Variation With Non-Isotropic Antennas

So far, we have assumed that the antenna patterns are isotropic. Now, consider non-isotropic antennas with far-field functions $g_0(\phi)$, and $g_1(\phi)$. When the two reference vehicles in Fig. 2 are on different lanes ($d_{\mathrm{y}} \neq 0$), the AOA varies depending on the speed and initial distance between the Tx and the Rx. This introduces variation in both the gain and phase of the far-field functions of antennas. In the following, we investigate the effects of these variations on the performance of ACN at medium to large distances. As was done in the previous sections, we study the effects of variation of antenna far-field functions while neglecting the effects of the two other quantities of interest ($\Omega$ and PL), by assuming that they remain constant over $KT$ s. That is, $\Omega(t) \approx b_{\Omega}$, $a_{\Omega} = 0$ in (13), and $\overline{A}(t) \approx b_{\mathrm{PL}}$, $a_{\mathrm{PL}} = 0$ in (32), when $0 \leq t \leq KT$. Then, we express the SNR of the $k^{\mathrm{th}}$ packet (6) in this case as

$$\gamma_k = \frac{P_{\mathrm{t}} b_{\mathrm{PL}}}{L\sigma_{\mathrm{n}}^2} \left| \sum_{l=0}^{L-1} |g_l(\phi_k)| \mathrm{e}^{-\jmath(\psi_l(kT) - \alpha_l kT)} \right|^2, \tag{46}$$

where the AOA is assumed to be constant over a packet duration $\phi(t) = \phi_k$, $kT \leq t \leq kT + T_{\mathrm{m}}$, $k = 0, 1, \ldots, K-1$, and so is $\psi_l$, $l = 0, 1$. Recalling that $\alpha_0 = 0$, and $\alpha = \alpha_1 \in \mathbb{R}$, the normalized sum-SNR can be expressed as

$$\frac{\sigma_{\mathrm{n}}^2}{P_{\mathrm{t}} b_{\mathrm{PL}}} \sum_{k=0}^{K-1} \gamma_k = \sum_{k=0}^{K-1} \sum_{l=0}^{1} \frac{|g_l(\phi_k)|^2}{2} + \sum_{k=0}^{K-1} |g_0(\phi_k) g_1(\phi_k)| \times \cos\big(\psi_1(kT) - \psi_0(kT) - \alpha kT\big). \tag{47}$$

From (5), it follows that for $k = 0, 1, \ldots, K-1$,

$$\begin{aligned} \psi_1(kT) - \psi_0(kT) &= \Omega(kT) - \underline{\angle g_1(\phi_k)} + \underline{\angle g_0(\phi_k)} - \beta \\ &= b_{\Omega} - \underline{\angle g_1(\phi_k)} + \underline{\angle g_0(\phi_k)} - \beta, \end{aligned}$$

since $\Omega_0(t) = 0$, $\Omega_1(t) = \Omega(t) = b_{\Omega}$ when $0 \leq t \leq KT$, $\beta_0 = 0$ and $\beta_1 = \beta \in [0, 2\pi)$. Unlike the case when antennas were assumed to be isotropic, we see here that the phase responses of non-isotropic antennas change with $\phi_k$, and introduce a time-varying phase shift. To analyze its effect, we apply an affine approximation taking into account the slow change of the AOA at medium to large distances (e.g., at $d_{\mathrm{x}} = 30$ m, $\phi$ changes by $9\,\mathrm{deg}/1$ s at most, when $\Delta_{\mathrm{v}} \in [-60, 60]$ km/h), following

$$\underline{\angle g_0(\phi_k)} - \underline{\angle g_1(\phi_k)} \approx b_{\mathrm{PH}} + a_{\mathrm{PH}} kT. \tag{48}$$

The coefficients $b_{\mathrm{PH}}$ and $a_{\mathrm{PH}}$ depend on the antenna patterns used and how fast the AOA changes. They can be obtained using the LS method or using the first-order Taylor series when an analytical formula for the antenna far-field functions is available. Adopting the above approximation, we can express the sum-SNR (47) as

$$S_{\phi}(x, y) = \sum_{k=0}^{K-1} \sum_{l=0}^{1} \frac{|g_l(\phi_k)|^2}{2} + J_{\phi}(x, y),$$

where

$$J_{\phi}(x, y) = \sum_{k=0}^{K-1} |g_0(\phi_k) g_1(\phi_k)| \cos(y - 2xk), \tag{49}$$

$x = (\alpha - a_{\mathrm{PH}})T/2$ and $y = (b_{\Omega} + b_{\mathrm{PH}} - \beta)$. The ACN initial phase shift $\beta$ can take any value in $[0, 2\pi)$, and so does $y$. Therefore, we assess the performance according to the worst-case sum-SNR

$$\inf_{y \in [0, 2\pi)} S_{\phi}(x, y) = \sum_{k=0}^{K-1} \sum_{l=0}^{1} \frac{|g_l(\phi_k)|^2}{2} + \inf_{y \in [0, 2\pi)} J_{\phi}(x, y). \tag{50}$$

When developing the ACN system under worst-case propagation assumptions in [7], [9], the signal direction $\phi_k$ was assumed to be negligibly varying over $KT$ s, and coinciding with the worst-case AOA defined as

$$\phi_{\min} = \arg \inf_{\phi \in [0, 2\pi)} \sum_{l=0}^{1} \frac{|g_l(\phi)|^2}{2}. \tag{51}$$

Thus, we can straightforwardly establish that when the AOA is varying, we achieve a gain in sum-SNR with respect to the worst-case scenario (i.e., $\phi_k = \phi_{\min}$, $\forall k$), since the first term in (50) satisfies

$$\sum_{k=0}^{K-1}\sum_{l=0}^{1}\frac{|g_l(\phi_k)|^2}{2} \geq \sum_{k=0}^{K-1}\sum_{l=0}^{1}\frac{|g_l(\phi_{\min})|^2}{2} = K\sum_{l=0}^{1}\frac{|g_l(\phi_{\min})|^2}{2}. \quad (52)$$

On the other hand, under worst-case assumptions of non-varying $\phi_k$ for $k = 0, \ldots, K-1$ (which implies that $a_{\rm PH} = 0$), we know that for $x = \alpha T/2 \in \mathcal{X}^\star$, $\inf_y J_\phi(x,y) = 0$. To investigate if this holds when the AOA is time-varying, and taking into account the slow change rate of $\phi$ at medium to large distances, we approximate using the LS or first-order Taylor series

$$|g_0(\phi_k)g_1(\phi_k)| \approx b_\phi + a_\phi kT, \quad (53)$$

where $b_\phi + a_\phi kT > 0$, $k = 0, 1, \ldots, K-1$. Following that,

$$J_\phi(x,y) = \sum_{k=0}^{K-1}|g_0(\phi_k)g_1(\phi_k)|\cos(y-2xk) \approx \sum_{k=0}^{K-1}(b_\phi + a_\phi kT)\cos(y-2xk). \quad (54)$$

From (54) we see that variation in $\phi$ has identical effects to PL variation effects captured by $J_{\rm PL}$ (36), and therefore they can be represented using the same loss function. Consequently, using the left-hand statement of Lemma 2 (41), and the definition (37), we deduce that

$$\inf_{y\in[0,2\pi)} J_\phi(x,y) < 0, \quad a_\phi \neq 0, x \in \mathbb{R}.$$

Therefore, when the AOA is time-varying, there is a loss in sum-SNR (50) (unlike the case when $\phi$ is fixed and where $\inf_y J_\phi(x,y) = 0$). The loss in sum-SNR is due to two factors. The first factor is the variation of the antenna gains $|g_0(\phi_k)g_1(\phi_k)|$, which results in a loss even if $a_{\rm PH} = 0$, $x = \alpha T/2 \in \mathcal{X}^\star$. This is identical to the effects of PL variation. The second factor is due to the variation of the phase response of antennas (48), which shifts the effective phase slope of ACN to $x = (\alpha - a_{\rm PH})T/2$, and introduces a loss in sum-SNR that has been studied in Section IV under time variation of $\Omega$.

In summary, the effects of time-varying AOA, with an affine approximation of the phase and magnitude responses of non-isotropic antennas, have the same model as the combined PL and $\Omega$ time variation model discussed in Section V-D. Therefore, we can readily conclude that the phase slope in $\mathcal{A}^\star$ that ensure a robust performance under the effects of time-varying far-field functions is given by (29). It is important to note that these conclusions are applicable for medium to large distances, where the affine approximations used in evaluating the sum-SNR loss term, $\inf_y J_\phi(x,y)$, are expected to be accurate. At short distances, despite that the characterizations of the loss term made in this section may not be very accurate, the gain term in sum-SNR indicated by (52) is still achieved. Furthermore, this gain is expected to be more noticeable at short rather than large distances, since the AOA change rate is much higher for the former case. These aspects are highlighted using an example of an antenna pattern in the numerical results section.

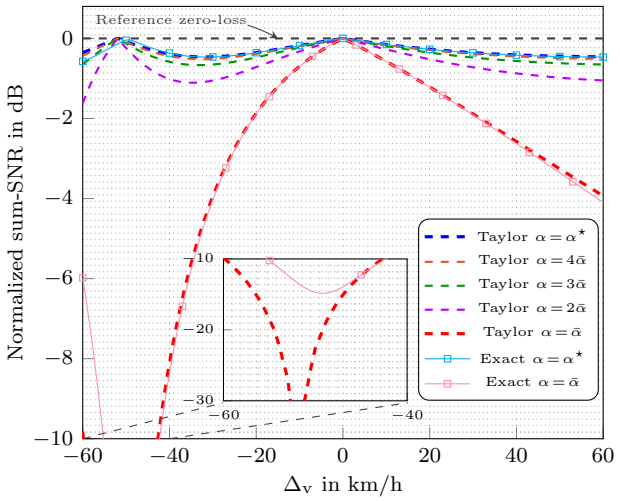


Fig. 9. Normalized worst-case sum-SNR under $\Omega$ variation $\big(1-L_\Omega(x)\big)$ in dB, for $K = 10$, $\delta_{\rm a} = 10\lambda$, $d_{\rm x} = 30$ m, and worst-case $d_{\rm y} \in \{-4, 4\}$ m. ($\bar{\alpha} = \frac{2\pi}{KT}$)

## VII. Numerical Results

In this section, we present numerical results corresponding to the normalized sum-SNR of a $1 \times 2$ ACN system (or equivalently a $2 \times 1$ ABN) when $\Omega$, PL, and $\phi$ vary over the duration of a burst of $K$ consecutive CAMs, $KT$ s. Throughout this section, we assume that the CAM broadcast period is $T = 0.1$ s and the burst length is $K = 10$ packets. This results in a maximum tolerable AoI of $KT = 1$ s (which is also used in other works, e.g., [22]).

### A. Sum-SNR Under Variation of $\Omega$

In the following, we visualize the sum-SNR for different choices of $\alpha \in \mathcal{A}^\star$, taking into account the time variation of $\Omega$ only. That is, the antennas are assumed to be isotropic, and the change in PL is assumed to be negligible over $KT$ s. The coefficients for the affine approximation of $\Omega$ in (13) are computed based on Taylor series expansion (14). The LS-based affine approximation was found to produce comparable results, and it is therefore omitted from the figures that follow in this subsection.

We recall that the worst-case normalized sum-SNR (22), is given by

$$\inf_{y\in[0,2\pi)} S_\Omega(x,y) = K\big(1 - L_\Omega(x)\big), \quad (55)$$

where $x = (\alpha - a_\Omega)T/2$. Since $a_\Omega$ (14) depends on $\Delta_{\rm v}, d_{\rm x}, \delta_{\rm a}$, and $d_{\rm y}$, we visualize the sum-SNR as a function of $\Delta_{\rm v}$ for a fixed initial distance $d_{\rm x}$, and a fixed antenna separation $\delta_{\rm a}$. Furthermore, since the effect of lateral distance results in $a_\Omega|_{-d_{\rm y}} = -a_\Omega|_{d_{\rm y}}$ (follows from (12), or (14)), the sum-SNR is minimized over $d_{\rm y} \in \{-4, 4\}$.

In Fig. 9, we plot the sum-SNR, after further normalization with respect to $K$, in dB, at a medium distance

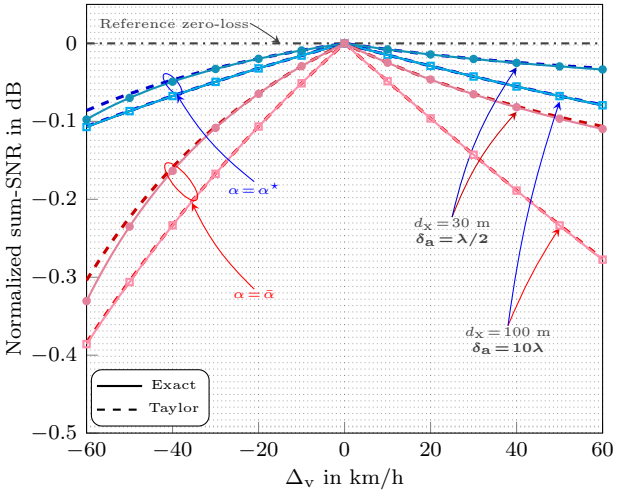


Fig. 10. Normalized worst-case sum-SNR under $\Omega$ variation $\big(1 - L_\Omega(x)\big)$ in dB, for $K = 10$, worst-case $d_y \in \{-4, 4\}$ m, $\delta_a = 10\lambda$ at $d_x = 100$ m, and $\delta_a = \lambda/2$ at $d_x = 30$ m. ($\bar{\alpha} = \frac{2\pi}{KT}$)

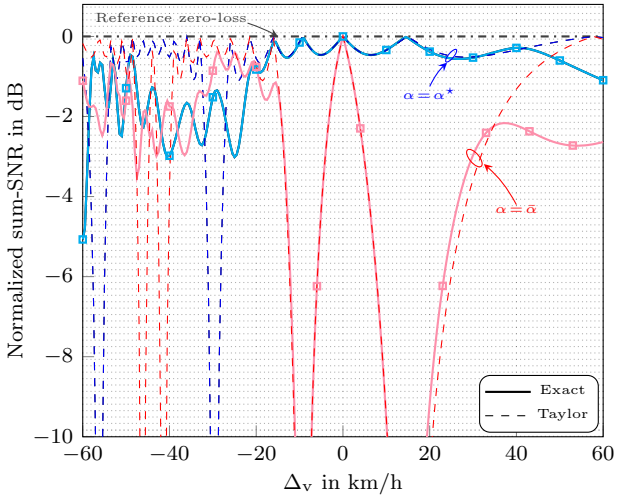


Fig. 11. Normalized worst-case sum-SNR under $\Omega$ variation $\big(1 - L_\Omega(x)\big)$ in dB, for $K = 10$, $\delta_a = 10\lambda$, $d_x = 10$ m, and worst-case $d_y \in \{-4, 4\}$ m. ($\bar{\alpha} = \frac{2\pi}{KT}$)

$d_x = 30$ m, when the antenna separation is $\delta_a = 10\lambda$. We recall that the loss function under variation of $\Omega$, $L_\Omega$ is symmetric around $\pi/2$ and therefore, we visualize the results only for $\alpha \in \mathcal{A}^\star$, $\alpha = q\frac{2\pi}{KT}$, $q = 1, \ldots, 5$. From Fig. 9, we see that the choice of $\alpha^\star = 5 \times 2\pi/KT$, which satisfies (29), exhibits a robust performance to channel phase variation with a low loss over the full range of $\Delta_v \in [-60, 60]$ km/h. Besides $\alpha^\star$, the choice of $\alpha = 4 \times 2\pi/KT$, or $\alpha = 3 \times 2\pi/KT$ results in comparably low loss too, which follows since the phase slopes have, respectively, the second and the third largest phase distances from the points of severe sum-SNR loss $x = q\pi$. The phase slope with the shortest phase distance from these points, $\bar{\alpha} = 2\pi/KT$, exhibits the highest loss, and it is the least robust phase slope in $\mathcal{A}^\star$. In Fig. 9, we also plot the sum-SNR using the exact value of $\Omega$ (12), for the most and the least robust choices of phase slopes in $\mathcal{A}^\star$ ($\alpha^\star$ and $\bar{\alpha}$). We see that the corresponding sum-SNR to the linear model matches the sum-SNR evaluated using the exact value of $\Omega$ for most speeds. The maximum loss experienced by $\alpha^\star$ when antennas are $\delta_a = 10\lambda$ apart is approximately 0.5 dB (according to the exact sum-SNR). If the antenna separation is smaller $\delta_a = \lambda/2$, then the ACN has a significantly lower sum-SNR loss for both $\alpha^\star$ and $\bar{\alpha}$ as can be seen in Fig. 10. In fact, the loss in sum-SNR of the ACN with $\delta_a = \lambda/2$ at $d_x = 30$ m is comparable to that of the ACN with $\delta_a = 10\lambda$ at a large distance $d_x = 100$ m. This suggests that implementing ACN systems with smaller antenna separation limits the sum-SNR loss caused by the time variation of $\Omega$. Note that, for both cases shown in Fig. 10, $\alpha^\star$ has an advantage over $\bar{\alpha}$, but the loss in sum-SNR is not significant for both phase slopes.

As explained in Section IV-A, modeling $\Omega$ as an affine function is valid for medium to large distances. Therefore, we are interested in evaluating the sum-SNR for short distances using the exact value of $\Omega$. In Fig. 11, we show the sum-SNR at $d_x = 10$ m when the antenna separation is $\delta_a = 10\lambda$. As expected, we see that at such a short distance, the affine model is accurate only for relatively low speeds $\Delta_v \in [-15, 35]$km/h. Note that the variation in $\Omega$ is faster for negative relative speeds than for positive speeds. This is because, in the case of negative speeds, the geometries between the Tx and the Rx change more dramatically due to decreasing distance between the VUs and potential overtaking movement. On the other hand, for positive speeds, the distance between the VUs is increasing, leading to a less severe change in geometries.

At high relative speeds, the change in $\Omega$ becomes much faster and cannot be approximated using a first-order polynomial. Following this, at the points $x = (\alpha - a_\Omega)T/2 = q\pi$, as it is the case for the ACN with $\alpha^\star$ at $\Delta_v \approx -30, -58$ km/h, the loss in sum-SNR is not as severe as it is predicted using the linear model. This is also observed at $\Delta_v = -41, -46$ km/h for $\bar{\alpha}$. This suggests that when the change in $\Omega$ is very fast to be accurately estimated using a linear approximation, the ACN/ABN system actually performs better than predicted by the linear model. It should be noted that at this short distance, $\alpha^\star$ shows an advantage compared to $\bar{\alpha}$ mostly when $\Delta_v > -15$ km/h.

To further emphasize the importance of a proper choice of $\alpha$, Fig. 12 displays the sum-SNR at a distance of $d_x = 10$ m, with antenna separation $\delta_a = \lambda/2$. We can see that with such a small antenna separation, the linear model is valid over a larger range of speed, even at this short distance. Moreover, the phase slope $\alpha^\star$ sustains a high level of performance across the full speed range compared to $\bar{\alpha}$.

### B. Sum-SNR Under PL Variation

To show the effects of PL variation and the performance of the different phase slopes, we plot in Fig. 13 the sum-SNR (38) for the worst-case $y$ as a function of $\Delta_v$ at a fixed medium distance $d_x = 30$ m. Both vehicles are on the same lane, $d_y = 0$ m, which results in non-varying $\Omega$ ($a_\Omega = 0$). Antennas are assumed to be isotropic. We normalize the sum-SNR with respect to the average path

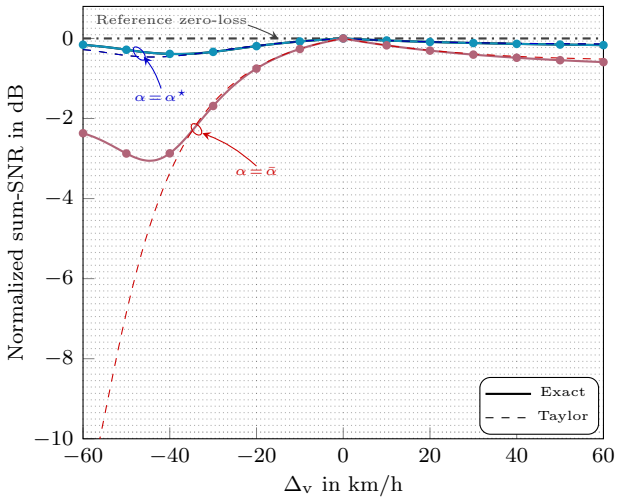


Fig. 12. Normalized worst-case sum-SNR under $\Omega$ variation $\big(1-L_\Omega(x)\big)$ in dB, for $K=10$, $\delta_a=\lambda/2$, $d_x=10$ m, and worst-case $d_y\in\{-4,4\}$ m. ($\bar{\alpha}=\frac{2\pi}{KT}$)

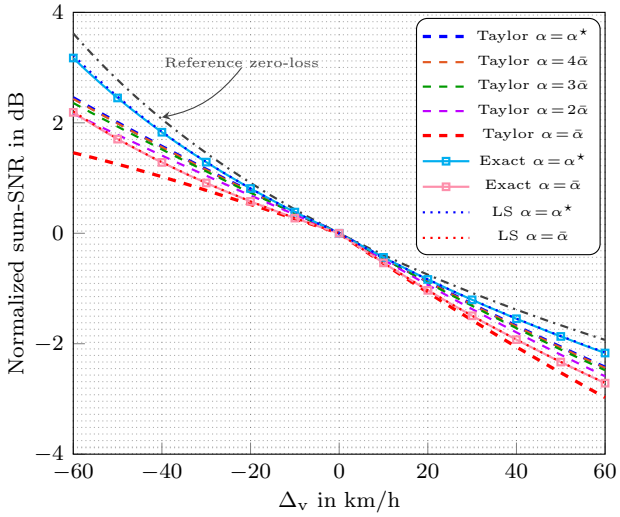


Fig. 13. Normalized worst-case sum-SNR under PL variation in dB, for $K=10$, $d_x=30$ m, and $d_y=0$ m. The PL model parameters correspond to WINNER+B1 model, and they are $d_{\text{ref}}=3$ m, $A_0=10^{5.32}$, $n_e=2.27$, and $\sigma_{\text{SH}}=3$. ($\bar{\alpha}=\frac{2\pi}{KT}$)

gain at $d_x=30$ m and with respect to $K$, such that it is equal to 0 dB at $\Delta_v=0$ km/h. We show the results for the affine approximation of the path gain, which is modeled according to WINNER+B1 model, based on both Taylor series (33) and the LS method, since the latter exhibited more accurate results in this case. From the figure, we observe that the loss due to PL variation is not significant for all phase slopes $\alpha\in\mathcal{A}^\star$. In particular, the loss is at most around 0.4 dB, and 1.5 dB, for $\alpha^\star T/2=\pi/2$, and $\bar{\alpha}T/2=\pi/K$, respectively (based on exact curves at $\Delta_v=-60$ km/h). The maximum loss of the remaining phase slopes within $\mathcal{A}^\star$ falls in between these two values. As discussed in Section V, unlike the effects of variation of channel phase, variation in PL does not shift the ACN/ABN phase slope, explaining the low loss in the sum-SNR.

### C. Sum-SNR Under Antenna Response Variation

In Section VI, we have seen that as $\phi$ varies, the phase and amplitude responses of antennas vary too. In Fig. 15, we show the sum-SNR (50) under these effects when the antennas employed by the ACN/ABN are those shown in Fig. 14. The sum-SNR is plotted as a function of $\Delta_v$ for a fixed $d_x$, and for the worst-case $y\in[0,2\pi)$, and worst-case $d_y\in\{-4,4\}$. The received signal is assumed to coincide with the worst-case AOA, $\phi_{\min}$ (51), at time $t=0$. Moreover, PL and $\Omega$ are assumed to be approximately constant over $KT$ s. The affine coefficients for the approximation of the far-field functions phase (48) and amplitude (53) are computed using the LS. For consistency, we normalize the sum-SNR with respect to $(|g_0(\phi_{\min})|^2+|g_1(\phi_{\min})|^2)$ and with respect to $K$, such that the sum-SNR equals 0 dB at $\Delta_v=0$ km/h.

From Fig. 15, we see that at a medium distance $d_x=30$ m, the loss in sum-SNR is low for $\bar{\alpha}$ and negligible for $\alpha^\star$ and the remaining phase slopes in $\mathcal{A}^\star$. Despite that the phase slopes are shifted by $a_{\text{PH}}$, resulting in $x=(\alpha-a_{\text{PH}})T/2$, the loss in sum-SNR is not as large as it was the case under time variation of $\Omega$ at $d_x=30$ m and $\delta_a=10\lambda$. The sum-SNR gain (52) due to the time-variation of $\phi$ is negligible at $d_x=30$ m for these antenna patterns, as can be inferred from the reference curve in Fig. 15 ($d_x=30$ m). However, at $d_x=10$ m, this gain is higher. On the other hand, the loss in sum-SNR due to $\inf_y J_\phi(x,y)$ is also higher at $d_x=10$ m compared to $d_x=30$ m, and it is most noticeable for $\bar{\alpha}$. This loss is largely caused by the phase deviation $a_{\text{PH}}$, which results in dips in sum-SNR, e.g., at $\Delta_v\approx 38$ km/h, when $x=(\bar{\alpha}-a_{\text{PH}})T/2=q\pi$. This can be concluded by examining the sum-SNR for $\bar{\alpha}$ when the phase response of the antennas is assumed constant over $KT$ s ($a_{\text{PH}}=0$). Unlike $\bar{\alpha}$, the phase slopes $\alpha^\star$ and $\alpha\in\{4\times 2\pi/KT, 3\times 2\pi/KT\}$ effectively reduce these effects and exhibit a low loss (approximately less than 0.5 dB) over the entire range of $\Delta_v$.

Although the linear model cannot be generally claimed to be accurate at short distances, we see from Fig. 15 that it correctly predicts the behavior of the sum-SNR curves, and it enables us to make a robust selection of a phase slope within $\mathcal{A}^\star$ (29) in mitigating the loss in sum-SNR due to the variation of antenna responses.

### D. Combined Effects of the Dominant Path Variation

In this section, we show the sum-SNR taking into account the combined effects of time-varying $\Omega$, PL, and $\phi$, i.e., a time-varying dominant path. The PL is modeled using WINNER+B1 channel model, and the receiver antennas have the patterns shown in Fig. 14. The received signal is assumed to coincide with the worst-case AOA, $\phi_{\min}$ at time $t=0$. To be able to compare the sum-SNR for different distances, we plot it without normalization. To that end, we set the transmitted power to $P_t=23$ dBm and the noise power at the receiver to $\sigma_n^2=-95$ dBm, which correspond to the commercial IEEE802.11p radio values (at 6 Mbit/s) [23]. In Fig. 16, we show the sum-SNR for worst-case $y\in[0,2\pi)$, and worst-case $d_y\in\{-4,4\}$, at $d_x\in\{10,30,100\}$.

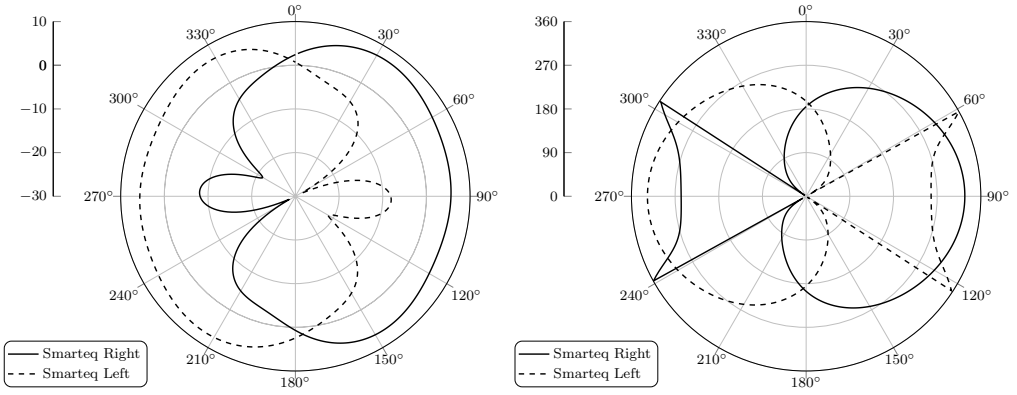


(a) Magnitude response $|g_l(\phi)|^2$ in dBi (b) Phase response $\angle g_l(\phi)$ in degrees

Fig. 14. Back-to-back patch antenna pattern. The antennas are designed by Smarteq[4] for Vehicular applications.

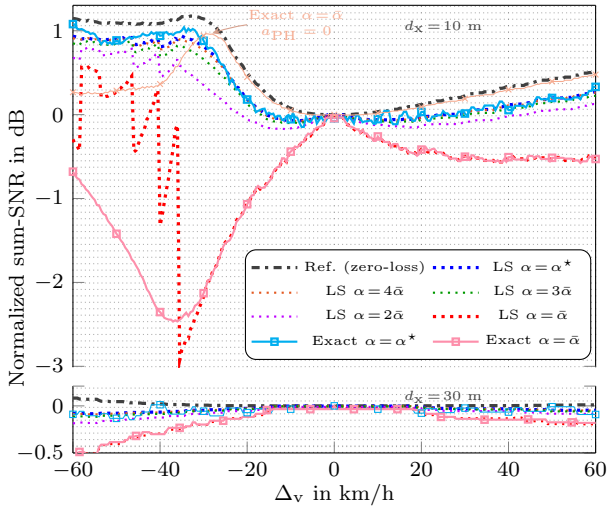


Fig. 15. Normalized worst-case sum-SNR under antenna response variation in dB, for $K = 10$, worst-case $d_y \in \{-4, 4\}$ m, $d_x = 30$ m, and $d_x = 10$ m. ($\bar{\alpha} = \frac{2\pi}{KT}$)

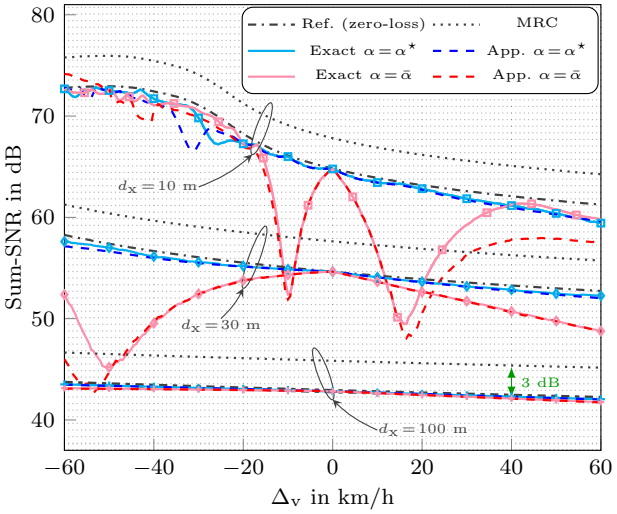


Fig. 16. Worst-case (non-normalized) sum-SNR under the variation of $\Omega$, PL, and AOA in dB, for $K = 10$, $\delta_a = 10\lambda$, worst-case $d_y \in \{-4, 4\}$ m, $P_t = 23$ dBm, and $\sigma_n^2 = -95$ dBm. The linear approximation coefficients of $\Omega$ and PL are computed using Taylor expansion, and those of antenna responses are computed using the LS. ($\bar{\alpha} = \frac{2\pi}{KT}$)

From the figure, we see that the observations made earlier when analyzing the effects of the three quantities separately are valid when taking into account their combined effects. Namely, ACN is impacted by time variation at medium and short distances. The choice of $\alpha^\star$ (29) yields a robust performance under time variation of the dominant path. Despite that $\bar{\alpha} = 2\pi/KT$ yields optimal performance under a non-time-varying dominant path (i.e., under worst-case assumptions), it can exhibit a severe loss in sum-SNR when the dominant path is time-varying, e.g., around 13 dB at $d_x = 30$ m, and around 16 dB at $d_x = 10$ m. Other choices of $\alpha \in \mathcal{A}^\star$ are more robust than $\bar{\alpha}$ and less robust than $\alpha^\star$. We recall that the antenna separation is set to $\delta_a = 10\lambda \approx 0.5$ m. Using lower $\delta_a$ decreases the loss for all $\alpha \in \mathcal{A}^\star$ and vice versa. In this paper, motivated by the low PL at short distances, we focused our analysis of ACN/ABN at medium to large distances. In Fig. 16, we see a visual validation of this approach where even under severe loss in sum-SNR, the system performance at $d_x = 10$ m is higher than the performance at $d_x = 100$ m and at $d_x = 30$ m for the major part of the speed interval.

As reported in [7], using a single digital port ACN yields a sum-SNR that is 3 dB lower than the sum-SNR achieved by a two-port MRC. Fig. 16 shows that ACN with the robust phase slope approximately maintains this 3 dB gap even under time-variation of the dominant path.

## VIII. Conclusions and Future Work

The ACN [7] and ABN [9] are robust multiple antenna schemes that maximize the sum-SNR of $K$ consecutive broadcast periodic packets under a worst-case propagation scenario. This corresponds to a single dominant path with non-varying AOA, PL, and phase shift between antennas $\Omega$ for $K$ packets. In this work, we investigated the performance of a $1 \times 2$ ACN ($2 \times 1$ ABN) when the three quantities of the dominant path are time-varying instead. The main findings of this work follow.

- The phase slopes that yield identical optimal sum-SNR when the AOA, PL, and $\Omega$ are non-varying,

[4]Smarteq Wireless AB, Sweden is a company specializing in antenna design and development for the vehicle industry and others.

yield different sum-SNR when any of these three quantities varies over the duration of $K$ packets.

- Time variation of $\Omega$ results in shifting the ACN phase slope and incurs a loss in sum-SNR that depends on the phase slope used, how fast the time variation of $\Omega$ is, and the antenna separation. In particular, the smaller the antenna separation, the less susceptible ACN is to these variations.
- To mitigate the loss in sum-SNR under the variation of $\Omega$ at medium to large distances, we proposed a design rule (29) that yields a phase slope that is robust against time variations and optimal under time-invariant conditions.
- Time variation of the PL does not induce a shift to the ACN phase slope, but it attenuates the sum-SNR achieved using any phase slope compared to the sum-SNR achieved under time-invariant conditions. The sum-SNR loss incurred is minor compared to the loss incurred due to the time variation of $\Omega$. The derived design rule (29) is found to yield a robust phase slope against variation of PL at medium to large distances, as well.
- Variation of the AOA induces a variation of the phase and amplitude of the antenna far-field functions, which has an equivalent effect to the combined $\Omega$ and PL time variation effects, with an extent that depends on the antennas employed. The design rule (29) yields a robust phase slope in $\mathcal{A}^\star$ in this case too.

In this study, we investigated the performance of ACN/ABN after relaxing the worst-case propagation scenario assumed when designing them. The next step is to study the performance of ACN/ABN under rich multipath propagation, which represents a full relaxation of the worst-case propagation assumption and is left for future work.

## APPENDIX

### A. Preliminaries

Here we present preliminary statements and lemmas that are used in the proof of Lemma 1 and Lemma 2.

Define the sets

$$\mathcal{X} \triangleq \{q\pi, q \in \mathbb{Z}\}, \tag{56}$$
$$\mathcal{X}^\star \triangleq \{q\pi/K, q \in \mathbb{Z}\} \setminus \mathcal{X}. \tag{57}$$

It follows that

$$x \in \mathcal{X} \iff x + \pi \in \mathcal{X}, \tag{58}$$
$$(\pi/2 - x) \in \mathcal{X} \iff (\pi/2 + x) \in \mathcal{X}. \tag{59}$$

The first statement follows since if $x \in \mathcal{X}$ then $x = m\pi$, $m \in \mathbb{Z}$ and hence $x + \pi = (m+1)\pi \in \mathcal{X}$. Similarly, if $(x + \pi) \in \mathcal{X}$ then $x + \pi = m\pi$, $m \in \mathbb{Z}$, and hence $x = (m-1)\pi \in \mathcal{X}$. To show (59), let $(\pi/2 \pm x) \in \mathcal{X}$, then $\pi/2 \pm x = m\pi$, where $m \in \mathbb{Z}$. Then multiplying both sides by $-1$ and adding $\pi$, we obtain $\pi/2 \mp x = (1-m)\pi$, hence $(\pi/2 \mp x) \in \mathcal{X}$.

For fixed positive integer $K > 1$ define the functions $f_1 : x \in \mathbb{R} \setminus \mathcal{X} \to \mathbb{R}$, and $f_2 : x \in \mathbb{R} \setminus \mathcal{X} \to \mathbb{R}$ following

$$f_1(x) \triangleq \frac{\sin(Kx)}{\sin(x)}, \tag{60}$$
$$f_2(x) \triangleq \frac{K\cos(Kx)}{\sin(x)} - \frac{\sin(Kx)}{\sin(x)}\cot(x). \tag{61}$$

**Lemma 3.** *Let $f_1$ be as defined in (60), then $|f_1(x)|$ and $f_1^2(x)$ are periodic with period $\pi$, and symmetric around $\pi/2$.*

*Proof.* From (60), and $\sin(K\pi) = 0$ it follows that

$$f_1(x+\pi) = \frac{\sin(Kx + K\pi)}{\sin(x+\pi)} = -\frac{\sin(Kx)\cos(K\pi)}{\sin(x)}.$$

Hence $|f_1(x+\pi)| = |f_1(x)|$ and $|f_1^2(x+\pi)| = |f_1^2(x)|$, and the periodicity property follows. To prove the symmetry property, we show that

$$|f_1(\pi/2 + x)| = |f_1(\pi/2 - x)|. \tag{62}$$

We have $|f_1(\pi/2 + x)|$ is given by

$$\left|\frac{\sin(K\frac{\pi}{2})\cos(Kx) + \cos(K\frac{\pi}{2})\sin(Kx)}{\cos(x)}\right|. \tag{63}$$

On the other hand, $|f_1(\pi/2 - x)|$ is given by

$$\left|\frac{\sin(K\frac{\pi}{2})\cos(Kx) - \cos(K\frac{\pi}{2})\sin(Kx)}{\cos(x)}\right|. \tag{64}$$

If $K$ is even, it follows from (63) and (64) that $|f_1(\pi/2 + x)| = |\sin(Kx)/\cos(x)| = |f_1(\pi/2 - x)|$. If $K$ is odd, it follows from the same equations that $|f_1(\pi/2 + x)| = |\cos(Kx)/\cos(x)| = |f_1(\pi/2 - x)|$. Hence $|f_1(x)|$ is symmetric around $\pi/2$. Since $f_1$ is a real-valued function, $f_1^2(x) = |f_1(x)|^2$, and thus $f_1^2(x)$ is symmetric around $\pi/2$ too, and the lemma follows. □

**Lemma 4.** *Let $f_2$ be as defined in (61), then $f_2^2(x)$ is periodic with period $\pi$, and symmetric around $\pi/2$.*

*Proof.* Employing trigonometric identities and noting that $\sin(K\pi) = 0$, we have

$$\begin{aligned} f_2(x+\pi) &= \frac{K\cos(Kx)\cos(K\pi)}{\sin(x+\pi)} \\ &\quad - \frac{\sin(Kx)\cos(K\pi)}{\sin^2(x+\pi)}\cos(x+\pi) \\ &= -\cos(K\pi) \\ &\quad \times \left(\frac{K\cos(Kx)}{\sin(x)} - \frac{\sin(Kx)}{\sin^2(x)}\cos(x)\right). \end{aligned} \tag{65}$$

Hence, $f_2^2(x+\pi) = (-\cos(K\pi))^2 f_2^2(x) = f_2^2(x)$, and thus $f_2^2(x)$ is periodic with period $\pi$. To prove the symmetry property, we first let $K$ be even. Using trigonometric identities and the fact that $\sin(K\frac{\pi}{2}) = 0$, we can express $f_2(\pi/2 + x)$ as

$$\frac{K\cos(K\frac{\pi}{2})\cos(Kx)}{\cos(x)} + \frac{\cos(K\frac{\pi}{2})\sin(Kx)}{\cos^2(x)}\sin(x),$$

and that is equal to $f_2(\pi/2 - x)$, when $K$ is even. Second, let $K$ be odd, then $f_2(\pi/2 + x)$ can be expressed as

$$-\frac{K\sin(K\frac{\pi}{2})\sin(Kx)}{\cos(x)} + \frac{\sin(K\frac{\pi}{2})\cos(Kx)}{\cos^2(x)}\sin(x),$$

while $f_2(\pi/2-x) = -f_2(\pi/2+x)$. Combining the cases, $K$ even and $K$ odd, we can conclude that $f_2^2(\pi/2+x) = f_2^2(\pi/2-x)$, and hence the symmetry property holds, and the lemma follows. □

### B. Proof of Lemma 1 and Lemma 2

We demonstrate the results of Lemma 1 and Lemma 2 together. To that end, for a fixed integer $K > 1$, $x \in \mathbb{R}$, and $y \in [0, 2\pi)$, define

$$J(x,y) \triangleq \sum_{k=0}^{K-1} (b + akT)\cos(y - 2xk), \tag{66}$$

where $(b + akT) > 0$, $k = 0, 1, \ldots, K-1$, implying that $b > 0$, and $a > -b/(K-1)T$. Moreover, define

$$L(x) \triangleq -\inf_{y\in[0,2\pi)} \frac{J(x,y)}{c_1 K}, \tag{67}$$

where $c_1 = (b + aT(K-1)/2) > 0$. For $b = b_{\text{PL}}$ and $a = a_{\text{PL}}$, (66) and (67), correspond to the functions $J_{\text{PL}}$ (36), and $L_{\text{PL}}$ (37), respectively. Similarly, for $b = 1$ and $a = 0$, (66) and (67) correspond to the functions $J_\Omega$ (19) and $L_\Omega$ (23), respectively.

To show the claims of Lemma 1 and Lemma 2 it is enough to show that for any $b > 0$ and $a > -b/(K-1)T$,

(i) $L(x)$ is given by

$$L(x) = \begin{cases} 1, & x \in \mathcal{X} \\ \sqrt{c_1^2 f_1^2 + c_2^2 f_2^2}/(c_1 K), & x \notin \mathcal{X} \end{cases} \tag{68}$$

where $c_2 = aT/2$, $f_1$, $f_2$ are defined in (60), (61), respectively, and $\mathcal{X}$ is defined in (56).
Note that when $b = 1$ and $a = 0$, $L(x) = |f_1(x)|/K$, $x \notin \mathcal{X}$.

(ii) $L(x)$ is periodic with period $\pi$ and symmetric around $\pi/2$.

(iii) $L(x)$ can be bounded as

$$\begin{cases} 0 < L(x), & a \neq 0 \\ 0 \leq L(x), & a = 0 \end{cases}, \quad L(x) \leq 1. \tag{69}$$

(iv) If $x \in \mathcal{X}^\star$, where $\mathcal{X}^\star$ is defined in (57), then

$$L(x) = \left| \frac{c_2}{c_1 \sin(x)} \right|. \tag{70}$$

Note that if $a = 0$, then $c_2 = 0$, $(c_1 \sin(x) \neq 0)$ and the lower bound in (69) is achieved, $L(x) = 0$.

(v) For $x \notin \mathcal{X}$, $L(x)$ can be bounded as

$$\frac{|f_1(x)|}{K} \leq L(x) \leq \frac{\sqrt{(K-1)^2 f_1^2(x) + f_2^2(x)}}{(K-1)K}. \tag{71}$$

Note that the lower bound is achievable when $a = 0$.

*Proof.* We start by deriving a different expression of $J$ that facilitates the proof of the lemmas. Let $x \in \mathcal{X}$, it follows that

$$J(x,y) = \cos(y) \sum_{k=0}^{K-1} (b + akT) = \cos(y) c_1 K. \tag{72}$$

Then, let $x \notin \mathcal{X}$. We can write

$$J(x,y) = b\ \mathrm{Re}\left\{ \mathrm{e}^{\jmath y} \sum_{k=0}^{K-1} \mathrm{e}^{-\jmath 2xk} \right\} + aT\ \mathrm{Re}\left\{ \mathrm{e}^{\jmath y} \frac{\jmath}{2} \frac{d}{dx} \sum_{k=0}^{K-1} \mathrm{e}^{-\jmath 2xk} \right\}. \tag{73}$$

Using the sum of the geometric series, we obtain

$$\sum_{k=0}^{K-1} \mathrm{e}^{-\jmath 2xk} = \mathrm{e}^{-\jmath(K-1)x} f_1(x),$$
$$\frac{d}{dx} \sum_{k=0}^{K-1} \mathrm{e}^{-\jmath 2xk} = -\jmath(K-1)\mathrm{e}^{-\jmath(K-1)x} f_1(x) + \mathrm{e}^{-\jmath(K-1)x} f_2(x),$$

since $f_2(x) = \frac{d}{dx} f_1(x)$. Substituting in (73) we arrive at

$$J(x,y) = \begin{cases} c_1 K\ \cos(y), & x \in \mathcal{X} \\ c_1 f_1(x)\ \cos\big(y - (K-1)x\big) & \\ \quad -c_2 f_2(x)\ \sin\big(y - (K-1)x\big), & x \notin \mathcal{X} \end{cases} \tag{74}$$

Now we tackle the lemmas claims.

(i) To show that $L(x)$ is given by (68), we first let $x \in \mathcal{X}$. Then, it follows from (74) that

$$L(x) = -\inf_{y\in[0,2\pi)} \frac{J(x,y)}{c_1 K} = -\inf_{y\in[0,2\pi)} \cos(y) = 1.$$

Second, let $x \notin \mathcal{X}$, and write

$$c_1 f_1(x) = R(x)\cos\big(\varphi(x)\big),$$
$$-c_2 f_2(x) = R(x)\sin\big(\varphi(x)\big),$$
$$R(x) = \sqrt{c_1^2 f_1^2(x) + c_2^2 f_2^2(x)},$$
$$\varphi(x) = \arctan\left( -\frac{c_2 f_2(x)}{c_1 f_1(x)} \right).$$

Then, it follows from (74) that

$$J(x,y) = R(x)\cos\big(y - (K-1)x - \varphi(x)\big),$$

and thus, when $x \notin \mathcal{X}$

$$-\inf_{y\in[0,2\pi)} \frac{J(x,y)}{c_1 K} = \frac{R(x)}{c_1 K} = \frac{\sqrt{c_1^2 f_1^2(x) + c_2^2 f_2^2(x)}}{c_1 K}.$$

where the minimizer is given by $y = \mathrm{mod}\big((K-1)x + \varphi(x) + \pi, 2\pi\big)$. Hence, (68) holds.

(ii) To show that $L$ is periodic and symmetric, let $x \in \mathcal{X}$, then from (68) we get $L(x) = 1$, which is a constant. Using (58) and (59) we can conclude that $L$ is periodic with period $\pi$, and symmetric around $\pi/2$ when $x \in \mathcal{X}$. The same statement is true when $x \notin \mathcal{X}$, since by (68) $L(x) = \sqrt{c_1^2 f_1^2(x) + c_2^2 f_2^2(x)}/(c_1 K)$, and since both $f_1^2$ and $f_2^2$ are periodic and symmetric as shown in Lemma 3 and Lemma 4, respectively.

(iii) To show (69), we first proof that $L(x) \leq 1$. To that end, observe that $\sum_{k=0}^{K-1}(b + akT) = c_1 K$. Then using (66) we deduce that

$$-c_1 K \leq J(x,y) \leq c_1 K. \tag{75}$$

Then, it follows that $L(x) = -\inf_y J(x,y)/(c_1 K) \leq 1$, which is achievable when $x \in \mathcal{X}$.

Second, to show the lower bounds in (69), we employ (68) and the fact that $c_1 > 0$ to deduce that

$$\begin{aligned} L(x) = 0 &\iff x \notin \mathcal{X} \\ &\iff \big(f_1^2(x) = 0, c_2^2 f_2^2(x) = 0\big). \end{aligned} \tag{76}$$

Since $f_1(x) = 0$ if and only if $x \in \mathcal{X}^\star$, and since

$$f_2^2(x) = \left(K \frac{\cos(Kx)}{\sin(x)}\right)^2 > 0, \quad x \in \mathcal{X}^\star, \tag{77}$$

we conclude that $0 < L(x)$ when $a \neq 0$, (since $c_2 = aT/2$), and $0 \leq L(x)$, when $a = 0$.

(iv) Let $x \in \mathcal{X}^\star$, from the definition (57) we deduce that $x = m\pi/K$, where $m \neq qK$, $q \in \mathbb{Z}$, hence $x \notin \mathcal{X}$. Substituting in (68), and recalling from the previous argument that $f_1(x) = 0$ we get

$$\begin{aligned} L(x) = \frac{|c_2 f_2(x)|}{c_1 K} &= \left| c_2 K \frac{\cos(m\pi)}{c_1 K \sin(x)} \right| \\ &= \left| \frac{c_2}{c_1 \sin(x)} \right|. \end{aligned} \tag{78}$$

(v) From (68) it follows that, for $x \notin \mathcal{X}$,

$$L(x) = \frac{1}{K} \sqrt{f_1^2(x) + \left(\frac{c_2}{c_1}\right)^2 f_2^2(x)}. \tag{79}$$

From the definitions of $c_1$ and $c_2$, we deduce that

$$\begin{aligned} \frac{c_2}{c_1} &= \frac{aT/2}{b + a(K-1)T/2} && (80) \\ &= \frac{1}{K-1} \frac{a/b}{a/b + 2/(K-1)T} && (81) \\ &= \frac{1}{K-1} \frac{w}{w + 2A}, && (82) \end{aligned}$$

where $w = a/b$ and $A = 1/(K-1)T$. From the condition $a > -b/(K-1)T$, we have that (82) is valid for $w > -1/(K-1)T = -A$.

We can now write, for $x \notin \mathcal{X}$,

$$\begin{aligned} L(x; w) &= \frac{1}{K} \sqrt{f_1^2(x) + g(w) \frac{f_2^2(x)}{(K-1)^2}} && (83) \\ &= \frac{\sqrt{(K-1)^2 f_1^2(x) + g(w) f_2^2(x)}}{K(K-1)}, && (84) \end{aligned}$$

where

$$g(w) = \left(\frac{w}{w + 2A}\right)^2, \qquad w > -A. \tag{85}$$

It is easily seen that for a fixed $x \neq \mathcal{X}$, $L(x; w)$ increases as $g(w)$ increases. Moreover, it is easily verified that

$$\begin{aligned} g(0) &= 0, \\ \lim_{w \to -A} g(w) &= \lim_{w \to \infty} g(w) = 1, \\ \frac{d}{dw} g(w) &= \frac{4Aw}{(w + 2A)^3} = \begin{cases} \leq 0, & -A < w \leq 0 \\ > 0, & w > 0 \end{cases} \end{aligned}$$

In other words, $g(w)$ is decreasing for $-A < w \leq 0$, attains its minimum as $w = 0$, and increases for $w \geq 0$. It follows that $\sup_{w > -A} g(w) = 1$ and $\inf_{w > -A} g(w) = 0$, and, therefore,

$$\begin{aligned} L(x; w) &\leq \sup_{w > -A} L(x, w) && (86) \\ &= \frac{\sqrt{(K-1)^2 f_1^2(x) + f_2^2(x)}}{K(K-1)}, && (87) \end{aligned}$$

and

$$L(x; w) \geq \inf_{w > -A} L(x, w) = \frac{|f_1(x)|}{K}. \tag{88}$$

Hence (71) holds.

All the claims have been shown and thus Lemma 1, and Lemma 2 follow. □

## REFERENCES


[1] S. Kaul, K. Ramachandran, P. Shankar, S. Oh, M. Gruteser, I. Seskar, and T. Nadeem, "Effect of antenna placement and diversity on vehicular network communications," in *Proc. 4th Annu. IEEE Commun. Soc. Conf. on Sensor, Mesh and Ad Hoc Commun. and Netw.*, June 2007, pp. 112–121.

[2] L. Ekiz, A. Posselt, O. Klemp, and C. F. Mecklenbräuker, "Assessment of design methodologies for vehicular 802.11p antenna systems," in *Proc. Int. Conf. on Connected Vehicles and Expo (ICCVE)*, Nov. 2014, pp. 215–221.

[3] O. Klemp, "Performance considerations for automotive antenna equipment in vehicle-to-vehicle communications," in *Proc. URSI Int. Symp. on Electromagn. Theory*, Aug. 2010, pp. 934–937.

[4] T. Abbas, J. Karedal, and F. Tufvesson, "Measurement-based analysis: The effect of complementary antennas and diversity on vehicle-to-vehicle communication," *IEEE Antennas and Wireless Propag. Lett.*, vol. 12, pp. 309–312, March 2013.

[5] T. Izydorczyk, F. M. L. Tavares, G. Berardinelli, M. Bucur, and P. Mogensen, "Performance evaluation of multi-antenna receivers for vehicular communications in live LTE networks," in *Proc. IEEE 89th Veh. Tech. Conf. (VTC2019-Spring)*, Apr.-May 2019.

[6] K. Maliatsos, L. Marantis, P. S. Bithas, and A. G. Kanatas, "Hybrid multi-antenna techniques for V2X communications—prototyping and experimentation," *Telecom*, vol. 1, no. 2, pp. 80–95, July 2020.

[7] K. K. Nagalapur, E. G. Ström, F. Brännström, J. Carlsson, and K. Karlsson, "Robust connectivity with multiple directional antennas for vehicular communications," *IEEE Trans. Intell. Transp. Syst.*, vol. 21, no. 12, pp. 5305–5315, Dec. 2020.

[8] C. B. Lehocine, E. G. Ström, and F. Brännström, "Hybrid combining of directional antennas for periodic broadcast V2V communication," *IEEE Trans. Intell. Transp. Syst.*, vol. 23, no. 4, pp. 3226–3243, April 2022.

[9] ——, "Robust analog beamforming for periodic broadcast V2V communication," *IEEE Trans. Intell. Transp. Syst.*, vol. 23, no. 10, pp. 18 404–18 422, Oct. 2022.

[10] A. Dammann and S. Plass, "Cyclic delay diversity: Effective channel properties and applications," in *Proc. IEEE Int. Conf. on Commun.*, Jun. 2007.

[11] S. M. Alamouti, "A simple transmit diversity technique for wireless communications," *IEEE J. on Sel. Areas in Commun.*, vol. 16, no. 8, pp. 1451–1458, Oct. 1998.

[12] *Intelligent Transport Systems Vehicular Communications; Basic Set of Applications; Part 2: Specification of Cooperative Awareness Basic Service,* document ETSI EN 302 637-2 V1.4.1, Jan. 2019.

[13] J. Daniel, C. Qi, and D. Luca, "Optimal data rate selection for vehicle safety communications," in *Proc. of the 5th ACM Int. Workshop on Veh. Inter-Networking*, Sept. 2008, pp. 30–38.

[14] R. Molina-Masegosa, J. Gozalvez, and M. Sepulcre, "Comparison of IEEE 802.11p and LTE-V2X: An evaluation with periodic and aperiodic messages of constant and variable size," *IEEE Access*, vol. 8, July 2020.

[15] S. Kaul, M. Gruteser, V. Rai, and J. Kenney, "Minimizing age of information in vehicular networks," in *Proc. IEEE Commun. Soc. Conf. on Sensor, Mesh and Ad Hoc Commun. and Netw.*, June 2011, pp. 350–358.

[16] T. Abbas, J. Karedal, F. Tufvesson, A. Paier, L. Bernado, and A. F. Molisch, "Directional analysis of vehicle-to-vehicle propagation channels," in *Proc. IEEE 73rd Veh. Technol. Conf. (VTC Spring)*, May 2011.

[17] A. F. Molisch, *Wireless Communication*, 2nd ed. NJ, USA: Wiley, 2011.

[18] *Study on LTE-based V2X Services; (Release 14),* document 3GPP TR 36.885 V14.0.0, June 2016.
[19] T. Abbas, K. Sjöberg, J. Karedal, and F. Tufvesson, "A measurement based shadow fading model for vehicle-to-vehicle network simulations," *Int. J. of Antennas and Propag.*, vol. 2015, June 2015.
[20] M. Gudmundson, "Correlation model for shadow fading in mobile radio systems," *Electron. Lett.*, vol. 27, no. 23, Nov. 1991.
[21] *D5.3: WINNER+ Final Channel Models*, document Wireless World Initiative New Radio–WINNER+, June 2010.
[22] M. E. Renda, G. Resta, P. Santi, F. Martelli, and A. Franchini, "IEEE 802.11p VANets: Experimental evaluation of packet inter-reception time," *Comput. Commun.*, vol. 75, pp. 26–38, 2016.
[23] F. Cure, "Cohda mobility MK5 module—datasheet," document V1.2.0, Cohda Wireless, Wayville, SA, Australia, May 2015.